IDENTIFICATION OF SYNTHETIC CYTOTOXIC INTERACTIONS TO IMPROVE THE EFFICACY OF DNA DAMAGING THERAPEUTIC AGENTS

by

Noushin Moshgabadi

B.Sc., Simon Fraser University, 2008

M.Sc., The University of British Columbia, 2010

A THESIS SUBMITTED IN PARTIAL FULFILLMENT OF

THE REQUIREMENTS FOR THE DEGREE OF

MASTER OF SCIENCE

in

THE FACULTY OF GRADUATE AND POSTDOCTORAL STUDIES

(Medical Genetics)

THE UNIVERSITY OF BRITISH COLUMBIA

(Vancouver)

January 2014

Abstract

Cancer therapies ideally selectively kill tumour cells and have little effect on normal cells. However, many current therapies are toxic to both tumour and normal cells. Differential killing can be achieved by exploiting the differences between tumour cells and normal cells. Tumour specific somatic mutations can be leveraged to affect selective killing by targeting secondary proteins required for the viability of mutant cancer cells. This rationale is called synthetic lethality (SL). Genome instability (GIN) genes, which are frequently mutated in tumours, are good candidates for finding SL interactions in combination with DNA repair enzyme inhibitors. If a somatically mutated GIN gene is involved in a DNA repair pathway, then inhibiting a second, parallel DNA repair pathway enzyme might trigger SL due to an inability to repair endogenous DNA damage. The combination of a GIN mutation and a DNA repair enzyme inhibitor would not be expected to result in SL in all cases. However, it may be possible that the combination of a GIN mutation and inhibition of a DNA repair enzyme could sensitize cells to low doses of a DNA damaging agent (DDA). We termed this phenomenon "synthetic cytotoxicity" (SC). The aim of my research was to discover and characterize SC relationships between GIN mutations found in tumours and loss of function of DNA repair enzymes, using *Saccharomyces cerevisiae* as a model experimental organism. I tested a matrix of 27 GIN mutations, three DNA repair enzyme mutations, and six different DDAs to test single and double mutants in the presence and absence of low concentrations of DDAs and discovered 6 SL interactions, 21 SC interactions, and surprisingly 19 cases of phenotypic suppression (PS). I also characterized the SC interaction between *tpp1Δ* and *mre11Δ* (homologous recombination defective) in response to bleomycin and revealed a crucial role for Tpp1 in the non homologous

endjoining DNA repair pathway. I propose a model in which the deletion of both Mre11 and Tpp1 inhibits the resection of bleomycin-induced double strand DNA breaks, resulting in unrepaired DNA damage and synthetic cytotoxicity.

Preface

This dissertation is original, unpublished work by Noushin Moshgabadi. Dr. Phil Hieter conceptualized this project, and Dr. Nigel O'Neil and Noushin Moshgabadi created the experimental design. Noushin Moshgabadi performed all the experiments, collected data and analyzed them, under the guidance of Dr. Phil Hieter and Dr. Nigel O'Neil.

Table of Contents

List of Tables

List of Figures

List of Abbreviations

AUC: Area Under the Curve

CC: Cancer Gene Census

CIN: Chromosome Instability

COSMIC: Catalogue of Somatic Mutations in Cancer

DDA: DNA Damaging Agent

DRE: DNA Repair Enzyme

DSB: Double Strand Break

F: Fitness

GC: Growth Curve

GIN: Genome Instability

Hereditary Nonpolyposis Colorectal Cancer (HNPCC)

HR: Homologous Recombination

MB: Methylene Blue

MMEJ: Microhomology-Mediated End Joining

MMR: Mismatch Repair

MMS: Methyl Methansulfonate

NA: Not Available

NER: Nucleotide Excision Repair

NHEJ: Non-Homologous End Joining

NI: No Interaction

NS: Not Sensitive

OD: Optical Density

PARP1: Poly (ADP-ribose) Polymerase-1

P-POD: Princeton Protein Orthology

PS: Phenotypic Suppression

S: Sensitive

SD: Standard Deviation

SGDP: Saccharomyces Genome Deletion Project

SL: Synthetic Lethality

TDP1: Tyrosyl-DNA-Phosphodiesterase

VLBNN: Very Large Budded Nucleus in the Neck

WT: Wild type

YPD: Yeast Extract Peptone Dextrose

Acknowledgements

I want to thank my supervisor, Dr. Phil Hieter, for having me in his laboratory and for giving me the opportunity to pursue this project in his laboratory. More importantly, he was a person who thought me to always “keep my chin up”. He is one of the few people who has had a huge impact on my life

I also want to thank Dr. Nigel O’Neil for his guidance and for reading and editing my thesis patiently. I appreciate the fact that he is a person who helps people without caring about his own benefits. I could not finish up this thesis without his help. In addition, I would like to appreciate the members of Hieter laboratory, Irene Barrett, Megan Filiatrault, Doris Vong, Peter Stirling, Supipi Duffy, Sean Minaker, Derek van Pel, Alina Chan, Hunter Li, Akil Hamza, Tejomayee Singh, Jan W. Stoepel, and Sidney Ang for being good lab mates.

I also want to thank my advisory committee, Dr. Elizabeth Conibear, and Dr. Michel Roberge, and examination committee Dr. Ann Rose and Dr. Leonard Foster for reading and commenting on my thesis.

The last but not the least, I want to thank my family specially my parents for supporting me and helping me in all stages of my life.

Chapter 1: Introduction

Changes in genome structure and sequence are associated with tumourigenesis (Charames & Bapat, 2003; Schvartzman et al., 2010). Cancer occurs in a multi-step mutational process in which cancer cell precursors accumulate genetic or epigenetic changes in a number of genes that can cause the cancerous state (Sjöblom et al., 2006; Vogelstein & Kinzler, 2004). Changes can occur by either germline or somatic mutations. Germline mutations are inherited from parents and are transmitted to offspring. Somatic mutations are acquired in subsets of cells during embryonic and postembryonic mitotic cell divisions. In cancer cells, somatic mutations fall into several different classes of DNA sequence changes. These include nucleotide substitutions of one base by another one; insertions or deletions of small or large segments of DNA; intra- or inter-chromosomal rearrangements, in which DNA has been broken and then religated to a DNA segment from elsewhere in the genome, and copy number increases or reductions. In addition, cancer cells might obtain completely new exogenous DNA sequences, especially from some specific viruses (Podlaha et al., 2012; Stratton et al., 2009). Epigenetic changes in somatic cells can alter gene expression by histone modification and DNA methylation. These genetic and epigenetic changes can produce three different classes of effects: 1) loss of function in tumour suppressor genes, 2) gain of function in oncogenes (Hahn & Weinberg, 2002; Hanahan & Weinberg, 2000; Vogelstein & Kinzler, 2004), and 3) mutations that cause genome instability (GIN). GIN mutations are important for initiation and progression of cancer (Cahill et al., 1999; Lengauer et al., 1997).

The genome maintenance system detects and resolves defects in DNA, and ensures that replication and segregation of chromosomes occurs accurately during cell division (Gatenby & Vincent, 2003; Douglas Hanahan & Weinberg, 2011; Loeb & Loeb, 2000). However, in

cancer cells, defects in the genome maintenance machinery increase the rates of mutation and DNA mis-segregation. Therefore, GIN mutations can cause mutator and chromosome instability (CIN) phenotypes that increase the chance of accumulating mutations, and aneuploidy in cancer cell precursors (Fishel et al., 1993; Kolodner et al., 2002; Leach et al., 1993; Lengauer et al., 1997; Negrini et al., 2010). Mutations in genes involved in the DNA damage response pathway can increase mutation rate and induce cancer. For example, loss of function of genes involved in mismatch repair (ie. *MSH2* and *MLH1*) increases the rate of spontaneous mutation that can eventually give rise to colon cancer (Kolodner, 1995). There is evidence that supports the idea that a CIN phenotype occurs early in cancer development increasing the rate of chromosome mis-segregation and plays an important role in cancer initiation (Rajagopalan et al., 2003; Shih et al., 2001). For example, mutations in both alleles of the mitotic spindle checkpoint kinase hBUB1B predispose patients to cancer, and provide support a link between aneuploidy and cancer development (Hanks et al., 2004).

GIN mutations in tumours differentiate tumour cells from normal cells. These mutations can be leveraged to affect differential killing by identifying Synthetic Lethal (SL) interactions. A SL interaction is defined when mutation in either of two genes alone is viable; however, mutations in both genes simultaneously are lethal (Figure 1). The protein product of a gene that, when mutant, displays a SL interaction with a known cancer mutation would be a good candidate for an anti-cancer drug target. This allows for the indirect targeting of non-druggable cancer mutations, and also generates selectivity since healthy cells lack the cancer specific mutations. There are at least four different mechanisms that can lead to a SL interaction: 1) two genes acting in essential redundant parallel pathways; 2) two hypomorphic mutations in genes belonging to the same essential pathway; 3) two uniquely redundant genes with respect to an

essential function can also induce SL; and 4) two subunits of an essential mutiprotein complex (Ferrari et al., 2010; Kaelin, 2005; Le Meur et al., 2008) .

Cancer is a disease that is often associated with defects in DNA repair. Whole genome sequence analysis has uncovered many tumour types that have mutations in genes involved in DNA repair pathways. Additionally, most tumour genome sequences elucidated so far have large numbers of somatic mutations, implying that there is an underlying GIN involved in cancer formation (Shaheen et al., 2011). Therefore, in cancer cells with a mutation causing GIN, a drug that inhibits the activity of a DNA repair enzyme could enhance genome instability to a lethal level (Figure 1) (Chan & Giaccia, 2011; Helleday et al., 2008). There are many DNA repair enzymes and many GIN genes involved in DNA repair pathways, and deletion of two parallel repair pathways might induce SL. Also, some GIN mutations can induce DNA damage; therefore, inhibiting DNA repair pathways could block the repair of this DNA damage thereby inducing SL (Stirling et al., 2012). For example, tumour cells defective in *BRCA1* or *BRCA2*-mediated homologous recombination (HR) repair are SL in combination with inhibition of the DNA repair protein, poly (ADP-ribose) polymerase-1 (*PARP1*) (Bryant et al., 2005; Farmer et al., 2005). Clinical trials also confirmed this interaction in cancer patients (Fong et al., 2009). In this case, endogenous DNA damage coupled with an inability to repair this damage by *PARP1* or the HR pathway results in increased genomic instability and cell death.

Not all GIN mutations are susceptible to DNA repair enzyme inhibitors. In such cases it may be possible to induce conditional synthetic lethality by sensitizing the tumours to exogenous DNA damage from treatment with a DNA damaging therapeutic agent, that could synergize with the DNA repair enzyme inhibitor and somatic GIN mutations present in tumour

cells. We are calling this specific case of conditional synthetic lethality ”Synthetic Cytotoxicity” (SC) (Figure 2). Currently, several clinical trials are assessing a similar strategy in which combination therapies of *PARP* inhibitors are administered together with low doses of DNA damaging agents (DDAs) such as, carboplatin, gemcitabine, and temozolomide (DNA alkylators), in BRCA-deficient tumours (Chan & Giaccia, 2011). Also, the sensitivity of tumour cells to alkylating chemotherapeutics increases in the absence of other DNA repair enzymes such as DNA polymerase β (Pol β), *O*-6-methylguanine-DNA methyltransferase (MGMT), N-methylpurine-DNA glycosylase (MPG), apurinic-apyrimidinic endonuclease 1 or flap endonuclease 1 (FEN1). Furthermore, suppression of REV3L, the catalytic subunit of Pol ζ, inhibits the error-prone DNA translesion synthesis (TLS), thereby sensitizing drug-resistant lung adenocarcinomas to cisplatin in murine models (Adhikari et al., 2008; Calabrese et al., 2004; Doles et al., 2010; Donawho et al., 2007; Evers et al., 2008; Rottenberg et al., 2008; Xie, Doles, Hemann, & Walker, 2010). All of these studies demonstrate that DNA repair enzyme inhibitors could be good candidates to sensitize tumour cells to DNA damaging agents (DDAs). However, most of these studies do not take into account the genotype of the targeted tumour. The aim of my project is to discover and characterize synthetic cytotoxic relationships between GIN genes mutated in tumours, DNA repair enzymes, and DNA damaging agents (Figure 3). The key to developing an effective combination therapy is to identify the combinations that increase the therapeutic index by increasing differential killing and reducing off-target toxicity.

Investigating the biological effects of DNA damage on the complex networks of genome instability genes in viable cells is critical to understanding the effects of the cancer treatment and the rationale-based design of therapeutic approaches. Each tumour contains a number of

driver and passenger mutations in addition to chromosome rearrangements and epigenetic changes that will affect the therapeutic response. Resistance to chemotherapeutic agents is often produced by either bypassing pathway deficiencies or by re-modeling the DNA damage response. Therefore, a comprehensive map of genetic interactions that determines SC interactions will establish an invaluable resource for the rational design of personalized therapy based on tumour genotypes.

To identify genetic interactions, we need a robust *in vivo* system with which to screen the combinations of GIN genes, DNA repair enzyme inhibitors and DNA damaging agents. By siRNA technology, one can screen genome-wide in mammalian cells to identify protein targets that when knocked down, cause lethality in combination with cancer mutations (Luo et al., 2009). However, this represents a labor and resource intensive approach. Since, the DNA damage response and mechanisms that ensure chromosomal stability are fundamental cellular processes, many genetic interactions between GIN genes and other genes are conserved across species (Kitagawa & Hieter, 2001; McLellan et al., 2009; McManus et al., 2009; Tarailo et al., 2007). For example, a SL interaction observed between *rad54Δ* and *rad27Δ* mutations in yeast was also conserved when *RAD54B* and *FEN1* were knocked-down in cancer cell lines (McManus et al., 2009). Furthermore, a yeast SL screen identified interactions between deletions of mismatch repair (MMR) components and DNA polymerases and this interaction was conserved in human cells as *MSH2*-deficient cells were SL with inhibition of DNA polymerase POLβ, and *MLH1*-deficient cells were SL with DNA polymerase POLδ inhibition (Shaheen et al., 2011). The yeast, *Saccharomyces cerevisiae*, can be used as a powerful model system for mining the large number of potential synthetic cytotoxic conditions. In *S. cerevisiae*, single and double mutant combinations can be easily constructed (Scherens & Goffeau, 2004).

Also, growth curves and spot assays can be used to quantify growth/fitness, and powerful experimental tools can be applied to discover the mechanisms causing specific phenotypes of interest. Using yeast we can apply high-throughput methods to explore SL or SC interactions.

To identify SC interactions, we started with a matrix of 81 yeast double mutants in which deletions or mutations in each 27 GIN genes was combined with a deletion in each of 3 DNA repair enzymes (Tdp1, Tpp1, Rad27) and treated with low doses of 6 different DNA damaging agents (Figure 3). The 27 GIN genes were chosen based on either orthology with CIN cancer genes, their involvement in DNA repair pathways, or that their deletion increased mutation rates in yeast (Table 2) (Cherry et al., 1998; Heinicke et al., 2007; Stirling et al., 2011). Tyrosyl-DNA-phosphodiesterase 1 (*TDP1*), DNA 3' phosphatase (*TPP1*) (*PNKP* in humans), and *RAD27* 5' flap endonuclease (*FEN1* in humans) were the three DNA repair enzymes that we chose because small molecule inhibitors have been, or are being, developed for the human orthologues of these enzymes (Freschauf et al., 2009; Huang et al., 2011; van Pel et al., 2013). In yeast, we can mimic inhibition of these three DNA repair enzymes (ie. *TDP1*, *TPP1*/*PNKP*, and *RAD27*/*FEN1*) using deletion mutants. Here is a brief description of each of these enzymes:

Tdp1: Tdp1 is involved in the repair of DNA lesions created by topoisomerase I and II poisoning. Tdp1 hydrolyzes 3' and 5'phosphotyrosyl bonds to remove protein-DNA adducts or to remove damaged nucleotides (Nitiss et al., 2006; Pouliot et al., 1999).

Tpp1: Tpp1 is the yeast ortholog of the 3' phosphatase domain of polynucleotide kinase (*PNKP*) in humans. Tpp1 removes 3' phosphates during DNA strand break repair (Boone et al., 2007).

Rad27: Rad27 is the yeast ortholog of human FEN1, which plays a role in lagging strand DNA replication, base excision repair, and the re-initiation of stalled replication forks (Liu et al., 2004).

The six DDAs were chosen from different categories of cancer therapeutic agents. Bleomycin was chosen from radiotherapy and radiomimetics group (double stranded DNA breaks), Methyl methanesulfonate (MMS) from monofunctional alkylator group, and cisplatin from bifunctional alkylator group, (intrastrand and interstrand crosslinks), camptothecin and etoposide were chosen as topoisomerase poisons, and hydroxyurea was applied as a replication inhibitor (Helleday et al., 2008).

Identification of SC interactions in yeast helps us to identify a small set of potential combination therapies that can be directly tested for conservation in mammalian cell culture. In addition, yeast provides a unique tool for subsequent analysis, including determining the mechanism of these interactions, and identification of other genes with potential SL or SC interactions by identification of genes with similar function (Van Pel et al., 2013). Therefore, the specific aims of my project are: 1) to identify synthetic cytotoxic interactions between genes commonly found mutated in tumours and DNA repair enzymes that selectively sensitize cells to low doses of DNA damaging agents in *S. cerevisiae,* and 2) to investigate the mechanism of action of some of the interesting interactions. In future, it will be of great interest to investigate the conservation of these interactions in mammalian tissue culture, and in animal models of cancer.

Chapter 2: Methods & Materials

2.1 Construction of single mutants in *S. cerevisiae*

All of the non-essential genes except *RAD1*, *RAD51*, *SGS1*, *MAD1*, and *MRE11* were obtained from the Saccharomyces Genome Deletion Project (SGDP), in which the open reading frames were replaced with *KanMx* selectable markers. Colony PCR was done according to the SGDP protocol on both wildtype and deleted strains with PCR primers that were positioned 200-400 bp from the start and stop codons of the gene of interest to confirm the existence of the deleted gene (Gietz et al., 1995) (http://www.yeastgenome.org/). Temperature sensitive (TS) alleles *cdc4-10*, *smc1-259*, and *scc2-4* were used for *CDC4*, *SMC1*, and *SCC2* essential genes, respectively. These TS alleles were fused to a *URA3* marker (McLellan et al., 2009). Direct transformation was used to replace *RAD1*, *RAD51*, *SGS1*, *MAD1*, and *MRE11* in the SGA query background with the *URA3* selectable marker (Gietz et al. 1995; Tong, 2001) (Table 1). BY4742 was used as the wild type strain.

2.2 Construction of double mutants in *S. cerevisiae*

Double mutants were generated by mating yeast strains containing deletions or mutations in GIN genes with DNA repair enzyme deletion mutants (Table 2). After tetrad dissection, viable or inviable double deletion haploids were obtained. Viable double mutants were then tested for SC under the application of low concentrations of six DDAs (Figure 4). Different measurements can be applied to quantify fitness and identify SC interactions. In this work, growth curve and spot assay analysis was used to measure the exponential growth rate of the mutant strains relative to each other and to that of wild type in the presence and absence of DDAs.

2.3 *S. cerevisiae* growth curve

All strains were grown overnight in Yeast Extract Peptone Dextrose (YPD) at 30°C

except for the temperature sensitive alleles, which were grown at 25°C. The cultures were diluted to an OD600 of 0.2 in fresh media in the morning, and allowed to grow for 4h in YPD, and were the diluted to an OD600 of 0.05 in fresh YPD in 96-well plates. Three different concentrations of DDAs in three replicates were applied to find a suitable concentration for the experiment; Bleomycin (1.25μg/ml, 2.5μg/ml, 2.75μg/ml), Hydroxyurea (150mM, 200mM, 250mM), Camptothecin (25μM, 50μM, 70μM), Cis-platin (1.2mM, 1.4mM, 1.6mM), Etoposide (1mM, 2mM, 3mM), and Methyl Methanesulfonate (MMS) (0.005%, 0.01%, 0.02%). The starting approximate concentration for each DDA was obtained from the literature, and the concentrations were adjusted by conducting growth curves to optimize the three different screening concentrations (Table 4, 5 & 6). M1000 (Tecan, Hillsborough, NC) plate reader was used to measure OD620 every 30 min for 24h or until the sample reached saturation (McLellan et al., 2009).

2.4 *S. cerevisiae* growth curve analysis

To calculate growth curve fitness, the strain fitness (F) was calculated by the area under the curve (AUC) and the fitness compared among the double mutants, the single mutants, and wild type (McLellan et al., 2012). For each mutant analyzed, there were at least three independent growth curves. The average AUC of these three independent growth curves with calculated standard deviation (SD) were converted to percentages, and scored as fitness percentage in Table 4, 5 & 6. The Product Model, a widely accepted mathematical model with the respect to fitness, was used to calculate the expected value, in which the fitness of double-mutants is the product of the corresponding single mutants fitness values (Boone et al., 2007; Dixon, Costanzo et al., 2009). Different interaction fitness scores were quantified by comparing expected double mutant fitness to the measured double mutant fitness.

2.5 *S. cerevisiae* spot assay analysis

The same procedure as in the "Growth Curve" section was used to prepare cells for spot assay analysis. The single and double mutant strains were added in fresh YPD to 96-well plates at an OD_{600} of 0.05, and then were serially tenfold diluted, and spotted onto YPD plates and YPD plus DDA plates in triplicate. Three different sub-lethal doses of each DDA were applied to obtain the optimal concentration. The growth of double mutants in the presence of DDAs was compared to single mutants.

2.6 Cell viability assay by methylene blue dye

Wild type, *tpp1Δ*, *mre11Δ*, and *tpp1Δ mre11Δ* strains were grown overnight on YPD medium. The cultures were diluted to an OD600 of 0.05 in the morning, and allowed to grow for 4h in YPD in the presence and absence of bleomycin for 3h. The cells (5ml) were centrifuged at 5,000rpm for 5 minutes, and the cells stained by re-suspension of the pellet in 4ml of 0.15mM methylene blue (MB) dye in 0.1 M phosphate buffer, pH7.4. After 6 minutes, the cells were collected by centrifugation, washed with 8ml of the same buffer and then re-suspended in 4ml of buffer (Bonora & Mares, 1982). The number of stained cells versus unstained cells were counted using a Haemocytometer by dropping 10ul of the sample at the edge of the coverslip and allowing it to run under the cover slip. The numbers of viable and dead cells were recorded. To obtain an accurate cell count, 40 to 70 dead cells were counted. The cell concentration was obtained by:

Cell concentration/ml = Average number of cells in one large square x dilution factor x 10^4 (https://www.hpacultures.org.uk/technical/ccp/cellcounting.aspx).

2.7 Microscopy

A strain with both the *RAD52-GFP* fusion gene (DNA damage foci marker) under the

control of its native promoter, and the *HTA2-RFP* tagged histone gene (nucleus marker) (see YNM373, Table 1) were crossed to obtain wildtype, *tpp1Δ*, *mre11Δ*, and *tpp1Δ mre11Δ* backgrounds containing both *RAD52-GFP* and *HTA2-RFP*. All the strains were grown overnight on SC media, then diluted and grown in the presence or absence of bleomycin for 3h. The number of Rad52-GFP foci was counted after 3h and the cell and nuclear phenotypes of all of the strains were examined under the microscope. Increases in Rad52 foci is an indication of increased DSBs (Alvaro, et al., 2007; Huh et al., 2003).

Live cells were mounted on concanavalin A coated slides and imaged with the GFP filter set (500 ms exposure) using a Zeiss axioscop and Metamorph software (Molecular Devices) essentially as described (Stirling et al., 2012). Images were analyzed using Image J (http://rsbweb.nih. gov/ij/index.html). Experiments were repeated in triplicate and the proportion of cells with nuclear staining and Rad52 foci was counted for at least 100 cells from each experiment.

2.8 Flow cytometry

The wild type, *tpp1Δ*, *mre11Δ*, and *tpp1Δ mre11Δ* yeast strains were grown overnight in liquid YPD at 30°C. The cultures were harvested and diluted to an OD600 of 0.3 in the morning, and allowed to grow for 1.5h in YPD. Alpha-factor was added to the cultures with OD of 0.2 and incubated at 30°C for 1.5-2h. Arrest was monitored by examining in the microscope for the absence of budded cells and the "shmoo" appearance in virtually all cells. The cultures were centrifuged, and rinsed with ice-cold YP (ie. YPD without dextrose). The OD of wild type, *tpp1Δ, mre11Δ, tpp1Δ mre11Δ* strains were adjusted to 0.15 by re-suspending them in YPD or YPD containing 2.5μg/ml bleomycin and incubated for 3h. Cells were centrifuged at 6500rpm for 2 minutes, and re-suspended in 1ml 0.2 M Tris pH 7.5 (twice). Then cells were fixed in 1ml

of 70% ETOH/0.2 M Tris PH 7.5 overnight at 4°C. Cells were re-centrifuged at 6500rpm for 2 minutes and re-suspended in 200µl of 1mg/ml RNAse/ 0.2M Tris PH 7.5, and incubated at 37 degrees for 1 hour. 20mg/ml Proteinase K was added to the solution for 1 hour, and finally 3µg/ml propidium iodide in 0.2M Tris PH 7.5 was added to the solution overnight at 4 degrees. The samples were sonicated prior to the FACS analysis. FSC-H versus FL3-H on the basis of alpha factor arrested controls was used to determine the percentage of cells with 1N DNA content in test samples. 20,000 cells were analyzed from each sample.

The numbers of the cells in G1, and G2/M were also counted by examining their morphology under the microscope after 3h in the presence and absence of bleomycin.

2.9 Plasmid strains & determination of recombination frequencies

The structures of the recombination reporter plasmids YCpHR and YCpL2 have been described in Sabourin et al, 2003 (Figure 14). Yeast strains (wild type, *tpp1Δ*, *mre11Δ*, *tpp1Δ mre11Δ* strains) were transformed with YCpHR or YCpL2 by selecting on SC-URA. Single colonies were grown overnight in SC-URA and the cultures diluted back and grown to an OD600 of 0.2 in the morning. The diluted yeast were split into parallel cultures of 2.5 ml, to which were added 5µg/ml bleomycin or an equivalent volume of SC-URA. Cultures were grown for 3h and dilutions from each culture were plated in duplicate on SC-URA for total cell viability, either on SC-URA + 60 mg/ml canavanine for selection of yeast carrying recombined YCpHR, or on SC-URA + 60 mg/ml canavanine + 10 mg/ml cycloheximide for selection of yeast carrying recombined YCpL2. Recombination frequencies were calculated for each drug treatment by dividing the number of recombinants/ml by the number of total viable cells/ml (Sabourin et al., 2003).

Chapter 3: Results

3.1 The components of the 27 X 3 X 6 test matrix for identifying SC interactions

To identify synthetic cytotoxic (SC) interactions, a matrix of 27 deleted or mutated yeast genome instability (GIN) genes in combination with 3 DNA repair enzyme gene deletions were treated with low doses of 6 different DNA damaging agents (DDA) (27 x 3 x 6). The 27 GIN genes chosen represented a wide range of biological activities including: cell cycle checkpoints, sister chromatid cohesion, nucleases, mRNA regulation, nucleosome remodeling, biosynthesis, and DNA repair pathways (Table 3) (Cherry et al., 1998). These 27 GIN genes were either the yeast orthologs of Chromosome Instability (CIN) cancer genes (Stirling et al., 2011), DNA repair pathway genes, or mutator genes (Cherry et al., 1998; Heinicke et al., 2007). Princeton Protein Orthology (P-POD) database was used to identify the human orthologs of these genes, and the Catalogue of Somatic Mutations in Cancer (COSMIC) and the Cancer Gene Census (CC) was used to confirm that many of these genes are frequently mutated in cancer (Forbes et al., 2010; Futreal et al., 2004) (Table 3). The three DNA repair enzymes, Tyrosyl-DNA-phosphodiesterase1 (Tdp1), DNA 3' phosphatase (Tpp1) (*PNKP* in humans), and 5' flap endonuclease (Rad27) (*FEN1* in humans), were chosen for analysis because small molecule inhibitors for these enzymes have been or are being developed for the human enzymes (Freschauf et al., 2009; Huang et al., 2011; van Pel et al., 2013). Inhibition of the DNA repair enzymes was mimicked by deletion alleles of the DNA repair enzymes in *S. cerevisiae.* DNA damaging agents were chosen from five different cancer therapeutic groups. Bleomycin was chosen as a radiomimetic (double stranded DNA breaks), methyl methanesulfonate (MMS) as a monofunctional alkylator, cisplatin as a bifunctional alkylator (intrastrand and interstrand

crosslinks), camptothecin and etoposide as topoisomerase poisons, and hydroxyurea as a replication inhibitor (Helleday et al., 2008) (Figure 3).

3.2 Identification of genetic interactions

To identify genetic interactions, different measurements can be taken to quantify fitness. Here, we grew single and double mutants in liquid media and measured OD over time to determine the exponential growth rate. The growth of the double mutant strains relative to that of single mutants and wild type in the presence and absence of DDAs was measured using Area Under the Curve, and converted to a percentage value. A genetic interaction was indicated by the deviation of a double mutant fitness (AUC percentage) from the predicted fitness based on the two single mutants. A double mutant with a fitness lower than predicted was called synergistic (Mani, et al., 2008). With respect to the fitness phenotype, we used a widely accepted mathematical model to calculate the predicted (or expected) value for the double mutant based on the Product Model. In the Product Model, the predicted fitness of the double mutant was the product of the observed single mutant fitness values (Boone et al., 2007; Dixon et al., 2009). Using these comparisons, all the interactions were classified into three groups: 1) No Interaction, 2) Synthetic Cytotoxicity, 3) Phenotypic Suppression (Suppression of Cytotoxicity). Suppression of cytotoxicity interactions were divided into two subgroups. In the first sub group were the double mutants that grew worse than either single mutants, but grew better than the expected value. These may represent weak suppressing interactions but for the purpose of this study they were considered to be no interaction (NI). In the second sub group were the double mutants that grew better than the worst single mutant; this group was called phenotypic suppression (PS) (Figure 5).

An example for each interaction with corresponding growth curves is shown in Figure 6. In the absence of a genetic interaction, the fitness of a double mutant was expected to be the product of the fitness of the two single mutants (Boone et al., 2007). For example, *tdp1Δ* mutants were no more sensitive to bleomycin (2.5 μg/ml) than wild type. However, an *mre11*Δ mutant showed a growth rate of 54% compared with a wild type strain at the same concentration of bleomycin. The *tdp1*Δ *mre11*Δ double mutant also showed the same growth rate (ie. 54%) in the presence of bleomycin as the *mre11*Δ mutant, thus, the genetic combination caused no enhancement or suppression of cytotoxicity (Figure 6A). SC interactions were observed when the fitness of a double mutant was lower than the predicted value. For example, *tpp1Δ*mutants had a growth rate of 108% compared to wild type in bleomycin (2.5 μg/ml). An *mre11*Δmutant was sensitive to bleomycin (2.5 μg/ml) with a growth rate of 65% of wild type. The double mutant, however, showed a growth rate of 41% compared to the wild type in the presence of bleomycin, such that the genetic combination caused a more severe phenotype than expected for the combination of *tpp1*Δand *mre11*Δ (expected *tpp1*Δ *mre11*Δ, 1.08* 0.65 = 0.70 or 70%) (Figure 6B). Phenotypic suppression occurred when the fitness of a double mutant was greater than the expected value. For example, *tpp1*Δ exhibited a growth rate of 105% compared to wild type in bleomycin (2.5μg/ml). *sgs1*Δ exhibited a growth rate of 28% of wild type in bleomycin (2.5 μg/ml). The double mutant, however, showed a growth rate of 75% in comparison to the wild type in bleomycin (2.5μg/ml), such that the genetic combination caused phenotypic suppression compared to the value expected for the combination of the *tpp1*Δ *sgs1*Δ (expected *tpp1*Δ *sgs1*Δ, 1.05*0.28=0.29 or 29%) (Figure 6C). For all of the SC and PS interactions, three different concentrations of DDAs in three replicates were applied to find a suitable (optimal) concentration for the experiments (described in section 2.3). The concentration chosen for

quantitative growth curve analysis (shown in Table 4, 5 & 6) was the concentration at which the largest difference was observed between the worst single mutant and the double mutant. The average area under the curve (AUC) of three replicates for each strain was calculated to determine the fitness of each strain. The observed fitness of a double mutant in the presence of specific DDA at an optimal concentration was compared to the expected fitness of a double mutant in the presence of DDA to determine PS or SC interactions (Table 4, 5 & 6).

3.3 Summary of the all of genetic interactions

Out of 486 potential interactions (27 x 6 x 3) that were analyzed, 440 showed no interactions (NI), 21 were synthetic cytotoxic (SC) interactions, 19 were phenotypic suppression (PS) interactions, and 6 were synthetic lethal (SL) interactions. In addition, 20/30 single mutants showed sensitivity to at least one of the DDAs that I used in this study. The results of all of the interactions are summarized in Figure 7. PS and SC interactions were classified according to presence of different DDAs. Red squares represent SC interactions and the green squares represent PS. The sensitivities of each single mutant to each DDA were represented by orange squares. SC interactions were most prevalent with the DDA bleomycin and with the DNA repair enzyme *TPP1*. One of the most interesting interactions was the SC interaction of *tpp1Δ mre11Δ* in the presence of bleomycin (2.5 μg/ml), since *MRE11* is highly mutated in colorectal, and several other cancers (Figure 7).

3.4 The SC interaction of *tpp1Δ mre11Δ* with bleomycin

The SC interaction of *tpp1Δ mre11Δ* with bleomycin (2.5 μg/ml) was observed both with growth curve (GC) and plate spot assays (Figure 9A&B). In the presence of bleomycin (2.5 μg/ml), the observed double mutant fitness of *tpp1Δ mre11Δ* in liquid medium was 41%

compared to the predicted value of 70% (Figure 9A), and *tpp1Δ mre11Δ* also grew very slowly on bleomycin (2.5 μg/ml) plates compared to single mutants and the wild type strain (Figure 9B).

To determine whether this SC interaction was the result of slow growth or cell death, methylene blue staining was used to measure cell viability. Viable cells can metabolize methylene blue, but dead cells cannot metabolize methylene blue and, as a result, the un-degraded methylene blue then colours the cells. Figure 9C shows that the number of dead cells increased dramatically after exposure to bleomycin for 3h. Therefore, the cell inviability assay showed that SC interaction of *tpp1Δ mre11Δ* with 2.5μg/ml bleomycin results in increased cell death.

3.5 Mechanism of SC of *tpp1Δ mre11Δ* with bleomycin

To gain insight about the mechanism of SC interaction of *tpp1Δ mre11Δ* with bleomycin, we conducted several phenotypic characterizations, including analysis of cell and nuclear morphology, cell cycle arrest, and the frequency of DSBs in *tpp1Δ mre11Δ* in the presence of bleomycin. In addition, we explored the nature of the DNA repair pathway defects in the Mre11 and Tpp1 mutant backgrounds.

3.5.1 Cell and nuclear morphology of *tpp1Δ mre11Δ* with 2.5μg/ml bleomycin

To investigate the mechanism underlying the SC of *tpp1Δ mre11Δ* with bleomycin, we examined the cell and nuclear morphology of single and double mutants in the presence and absence of bleomycin to determine whether the cell cycle arrest represented by large number of budded or unbudded cells induced SC. Wild type, *tpp1*Δ*, mre11*Δ*,* and *tpp1*Δ *mre11*Δ cells expressing Hta2-RFP histone were examined for nuclear morphology, in the presence and absence of bleomycin. Both *mre11*Δ and *tpp1*Δ *mre11*Δ with and without bleomycin show a Very Large Budded Nucleus in the Neck (VLBNN) phenotype (Figure 10 A&B). However, the

percentage of VLBNN phenotype was dramatically increased in double mutants with bleomycin (Figure 10B). The VLBNN phenotype occurs in medial nuclear division arrested cells (Samejima, et al., 1993). Thus, in the next step, we tried to investigate whether this VLBNN phenotype was the consequence of cell cycle arrest.

3.5.2 Cell cycle arrest of *tpp1Δ mre11Δ* with 2.5μg/ml bleomycin

Flow cytometry was used to analyze the cell cycle of wild type, *tpp1Δ*, *mre11Δ*, and *tpp1Δ mre11Δ* cells in the presence and absence of bleomycin after release from G1 arrest by alpha factor (Figure 11A). The percentage of cells in the G1, and G2/M stages were also counted by observing the morphology of yeast cells under the microscope after 3h with and without the presence of bleomycin (Figure 11B). Both flow cytometry and cell morphology showed *mre11*Δ and *tpp1*Δ *mre11*Δ accumulated at the G2/M stage in the presence of bleomycin (Figure 11A & B).

3.5.3 Frequency of DSBs in *tpp1Δ mre11Δ* mutants treated with bleomycin

Since both Mre11 and Tpp1 are involved in DNA repair pathways, one possibility is that the *tpp1*Δ *mre11*Δ cells could not repair the bleomycin-induced DSBs, and as a consequence the *tpp1*Δ *mre11*Δ cells arrested and died. To test this hypothesis, we measured the frequency of Rad52 foci, which are indicative of DSBs, after bleomycin treatment in *tpp1Δ mre11Δ* compared to wild type and the single mutants. Increases in Rad52 foci indicated an increase in DSBs or recombination intermediates. The *RAD52 GFP* fusion gene under the control of the Rad52 native promoter was introduced into wild type, *tpp1*Δ, *mre11*Δ, and *tpp1*Δ *mre11*Δ cells, and Rad52 foci were counted. In the absence of bleomycin, 1.8%, 1%, 12.8%, and 16.2% of cells showed Rad52 foci respectively; however, in the presence of bleomycin, 8.7%, 5.1%, 13.9% and 25.6% of cells showed Rad 52 foci, respectively. Therefore, the frequency of cells

with Rad52 foci is dramatically increased in *tpp1*Δ *mre11*Δ in the presence of bleomycin (Figure 12B). Rad52p is essential for homologous recombination (HR), and is one of the major proteins involved in the repair of DNA lesions, especially double strand DNA breaks. Therefore, this increase might be due to increased frequency of DSBs, inefficient resolution of recombination intermediates, or hyper-recombination. Also, most of the cells with Rad52 foci also exhibited the VLBNN phenotype suggesting that the VLBNN phenotype correlated with the presence of unrepaired DNA damage (Figure12C).

3.5.4 Identification of Mre11 and Tpp1 DNA repair pathways

The reason for the SC interaction of *tpp1*Δ *mre11*Δ in the presence of bleomycin is likely due to unrepaired DSBs produced by bleomycin. The main two DNA repair pathways to repair DSBs are homologous recombination (HR), and non-homologous end joining (NHEJ). To determine which pathways were compromised in the single and double mutants, we deleted components of the two main DNA repair pathways to repair DSBs (HR and NHEJ), in combination with *tpp1*Δ or *mre11*Δ and in the presence of bleomycin to identify which DNA repair pathways were responsible for the SC interaction of *tpp1*Δ *mre11*Δ with bleomycin. We chose *RAD52*, *RAD51*, *RAD50* and *XRS2* genes as essential genes for HR, and *YKU70*, *LIF1*, *DNL4* as essential genes for NHEJ. According to our model, deletions of the two main DNA repair pathways in the presence of DSB should induce SC. Thus, deletion of the *RAD52* gene which blocks the HR pathway and deletion of *YKU70* gene which blocks the NHEJ pathway in the presence of bleomycin should induce SC (Figure 13A); this SC interaction was shown by both growth curve and spot assay (Figure 13B). The results of the combination of *tpp1Δ* or *mre11Δ* with deletions of HR or NHEJ pathways are summarized in Figure 13C. Deletion of *YKU70* and *RAD52* in the presence of bleomycin induced SC since *yku70Δ* is deficient for NHEJ

and *rad52Δ* is deficient for HR and the DSBs induced by bleomycin could not be repaired. Similarly, deletion of *MRE11* (HR pathway) and *YKU70* (NHEJ pathway) caused SC in the presence of bleomycin. Deletion of *XRS2* (HR pathway) and *TPP1* in the presence of bleomycin induced SC. In contrast, *tpp1Δ* showed no genetic interaction with *yku70Δ*, *lif1Δ*, or *dnl4Δ* (NHEJ pathway) in the presence of bleomycin. Therefore, Tpp1 could be involved in NHEJ pathway since deletion of the two repair pathways HR and NHEJ induces SC in the presence of bleomycin, and *tpp1Δ* was SC with deletion of HR genes but showed no interactions with deletions of NHEJ genes. Based on my genetic interaction data, *tpp1Δ* appears to function in the NHEJ pathway and loss of both Tpp1 and the HR component Mre11 result in deficiencies in both HR and NHEJ, which result in SC to bleomycin-induced DSBs.

3.5.5 Application of YCpHR and YCpL2 plasmids to estimate the rate of HR and NHEJ respectively

To test this hypothesis further, we used plasmids that allowed measurement of the frequency of HR and NHEJ respectively in the presence and absence of bleomycin in single and double mutants. Wild type, *tpp1Δ*, *mre11Δ*, *tpp1Δ mre11Δ* cells were transformed with YCpHR and YCpL2 plasmids (Sabourin et al., 2003) (Figure 14). YCpHR is a plasmid that contains the canavanine sensitivity gene (*CAN1*) flanked on both sides by a copy of *LEU2* gene. Homologous recombination between the *LEU2* direct repeats results in deletion of *CAN1* gene, which can be scored by the ability of cells to grow in the presence of canavanine (Figure 14B). YCpL2 plasmid was used to monitor non-homologous end-joining events. YcpL2 carries a cycloheximide sensitivity gene, *CYH2*, in place of one of the two *CAN1* genes in YCpHR, in the opposite orientation to the *CAN1* gene. Non-homologous recombination can be scored by the ability to grow in the presence of both cycloheximide and canavanine (Figure 14A) (Sabourin et

al., 2003). Figure 14A shows that the rate of NHEJ reduced dramatically when *TPP1* was deleted in both the presence and absence of bleomycin. Figure 14B shows that the rate of HR reduced when *MRE11* was deleted in the presence or absence of bleomycin. Therefore, we could conclude that deletion of *TPP1* is required for NHEJ and that Mre11 is required for HR; thus, the DSBs induced by bleomycin in the *tpp1Δ mre11Δ* double mutants could not be repaired by HR or NHEJ and resulted in SC**.**

Chapter 4: Discussion

4.1 Identification of SC Interactions and expanding the number of conditional SL interactions

The aim of this project was to identify synthetic cytotoxic interactions between mutations commonly found in tumours, DNA repair enzymes, and DNA damaging agents. Synthetic cytotoxicity is a sub-class of conditional synthetic lethality, when a synthetic lethal interaction is observed under a specific condition. In the case of synthetic cytotoxicity the condition is the application of agents that cause DNA damage, which results in increased cytotoxicity. SC expands the potential for genetic interactions beyond synthetic lethality. I tested 27 gene mutations for SL with mutations affecting three DNA repair enzymes (81 combinations) and found 6 SL interactions. By adding low concentrations of different DNA damaging agents to the viable double mutants, the number of genetic interactions was extended by an additional 21 examples. Therefore, we can expand the number of genetic interactions by adding low concentrations of DDAs to enhance gene-gene interactions to a significant extent.

4.2 The deleted or mutated genes or DDAs that showed the highest numbers of SC interactions

Among the three deleted DNA repair enzyme genes, *rad27Δ* was the only DNA repair enzyme deletion that showed SL interactions. *rad27Δ* also had the highest number of SC interactions in combination with the different DDAs and the query genes (ie. 11 SC interactions out of 21 SC interactions). These results are not unexpected as Rad27 plays important roles in DNA replication and repair (Balakrishnan & Bambara, 2013), and loss of Rad27 results in a slow growth phenotype in yeast and deletion of its ortholog, *FEN1*, in the mouse results in embryo lethality (Larsen et al., 2003). Fewer SC interactions were observed with *tdp1Δ* and *tpp1Δ*. This

may be due in part to the fact that both *tdp1*Δ and *tpp1Δ* are more fit than *rad27Δ* and grow at the same rate as wild type.

4.2.1 Interactions with the RecQ helicase mutant Sgs1

sgs1Δ shows many interesting interactions in combination with the three repair enzyme inhibitor mutants. *sgs1Δ rad27Δ* is SC in the presence of three different DDAs; bleomycin, etoposide, and MMS. This is consistent with previous research demonstrating that showed that the *sgs1Δ rad27Δ* double mutants are sensitive to MMS and other DDAs (Ringvoll et al., 2007). In contrast, *sgs1Δ* in combination with *tdp1Δ* in the presence of bleomycin or MMS, and *sgs1Δ* in combination with *tpp1Δ* in the presence of bleomycin resulted in phenotypic suppression of the sensitivity of *sgs1Δ*. This suggests that Tdp1 and Tpp1 are required for the sensitivity of *sgs1Δ* to certain DDAs.

4.2.2 Interactions with *tdp1Δ*

The SC interaction of *rad1Δ* or *rad10Δ* in combination with *tdp1Δ* in the presence of camptothecin was observed before (Vance & Wilson, 2002). Rad1 and Rad10 form a structure-specific endonuclease required for the cleavage of certain DNA flap substrates. Vance and Wilson hypothesized that Tdp1 and Rad1/Rad10 function in parallel pathways to repair TopI-mediated replicative damage caused by the TopI poison camptothecin. Blocking the two parallel pathways prevented the repair of TopI replicative damage and thus resulted in increased sensitivity to camptothecin. We also observed a SC interaction of *tdp1Δ* in combination with *mlh1Δ* in the presence of both bleomycin and cisplatin; however, in the presence of hydroxyurea PS was observed. Since Mlh1 is required for mismatch repair, and germ-line mutations in this gene predispose to hereditary nonpolyposis colorectal cancer (HNPCC), further investigation on this interaction might be beneficial (Shaheen et al., 2011).

4.2.3 Interactions with *tpp1Δ*

Five out of six interactions of *tpp1Δ* with GIN mutations were in response to the application of a low dose of bleomycin. Also, among the six DDAs that we used, the highest numbers of SC interactions were observed in the presence of bleomycin. Therefore, the SC interactions of *tpp1Δ* and GIN deleted genes in the presence of bleomycin are noteworthy. I further investigated the SC interaction of *tpp1Δ mre11Δ* in the presence of low doses of bleomycin. *MRE11* is frequently mutated in different types of cancer especially colon cancer. Tpp1 is homologous to the 3' phosphatase portion of the human protein PNKP (Vance & Wilson, 2001), and a small molecule inhibitor was identified for human PNKP. PNKP is a potential target for increasing the sensitivity to chemotherapeutic agents such as bleomycin and camptothecin (Bernstein et al., 2008).

4.3 The mechanism of *tpp1Δ mre11Δ* SC interaction under the application of bleomycin

The SC interaction of *tpp1Δ mre11Δ* in the presence of bleomycin was demonstrated by both growth curve and spot assay. The methylene blue assay indicated that both a slow growth phenotype and cell death were responsible for the reduced fitness. To investigate further the mechanism underlying this SC interaction, we examined the cellular and nuclear morphology of *tpp1Δ mre11Δ* cells after treatment with bleomycin. Both *mre11Δ* and *tpp1Δ mre11Δ* exhibited a Very Large Budded Nucleus in the Neck (VLBNN) phenotype when treated with a low dose of bleomycin. However, the effect was far stronger in *tpp1Δ mre11Δ* cells. This phenotype is similar to that observed in cells treated with high level of ionization radiation, which generates DSBs that must be repaired before mitosis; therefore, the cell cycle is arrested at G2/M stage to allow time for DNA repair resulting in the VLBNN phenotype. This cell cycle arrest is mediated by the checkpoint proteins Rad9 (Weinert & Hartwell, 1990). A VLBNN phenotype is also

observed in *cnm67Δ* cells, which have a defective mitotic spindle and can not resolve mitotic nuclear migration (Schaerer et al., 2001). In *S. cerevisiae*, nuclear migration consists of two major steps. In the first step, the nucleus moves from a random position in the mother cell to a location close to the bud neck in S-phase. In the second step insertion of the elongating and separating nucleus into the daughter cells during anaphase occurs in M phase (Schaerer et al., 2001).

By observing the VLBNN phenotype in both *mre11Δ* and *tpp1Δ mre11Δ* in response to bleomycin, we can conclude that the nuclear migration was arrested after the first stage of nuclear migration; Flow cytometry of *mre11Δ* and *tpp1Δ mre11Δ* cells after the application of bleomycin, and examination of the morphology of the *mre11Δ* and *tpp1Δ mre11Δ* cells under the microscope, confirmed that the cells were arrested at the G2/M stage. To determine if the G2/M arrest was due to unrepaired DNA damage, I measured the frequency of cells with Rad52 foci. Rad52 is essential for homologous recombination and the organization of repair centers in response to DSBs. Increases in the frequency of cells with Rad52 foci can indicate increased DSBs, or defects in completion of recombination. Consistent with increased DNA damage resulting in G2/M arrest, the number of cells with Rad52 foci increased in both *mre11Δ* and *tpp1Δ mre11Δ* in the presence of bleomycin. The frequency of cells with Rad52 foci was greatest in *tpp1Δ mre11Δ* in the presence of bleomycin. Therefore, it is likely that the DSBs produced by bleomycin could not be efficiently repaired in *tpp1Δ mre11Δ* cells and as a result caused G2/M arrest and death.

Two different DNA repair pathways can repair DSBs. There are two possible explanations for the SC of *tpp1Δ mre11Δ* to bleomycin: 1) Tpp1 has an as yet un-discovered function in NHEJ and the loss of both NHEJ and HR (from a mutation in *MRE11*) can inhibit the

repair of DSBs and induce SC, or 2) Tpp1 functions in HR and loss of Tpp1 enhances the HR-defects of the *mre11* mutant. To test these hypotheses, I examined the effect of bleomycin on viability of cells after blocking both repair pathways by eliminating an essential gene in each pathway. A SC interaction was observed in *rad52Δ* (HR deficient) and *yku70Δ* (NHEJ deficient) double mutants in the presence of bleomycin confirming that loss of HR and NHEJ results in SC to bleomycin. Then, I examined the SC interaction of *tpp1Δ* or *mre11Δ* in combination with the deletion of genes essential for HR or NHEJ in the presence of bleomycin. The deletions of NHEJ-essential genes in combination with *mre11Δ* in the presence of bleomycin caused SC. This indicates that Mre11 has an essential role in the HR pathway. The deletion of *MRE11*, which is essential for HR in combination with *tpp1Δ* in the presence of bleomycin caused SC. However, the deletion of NHEJ-essential genes in combination with *tpp1Δ* in the presence of bleomcyin caused no genetic interaction. These assays suggested that Tpp1 has a role in NHEJ that has not been previously described. To look more specifically at the contributions of HR and NHEJ, I used a plasmid assay to measure the rates of HR and NHEJ and found that loss of *MRE11* resulted in a dramatic reduction of HR but not NHEJ in both bleomycin-treated and untreated cells consistent with Mre11's expected role in HR. When I assayed HR and NHEJ in the *tpp1* mutant the rate of NHEJ is reduced but the rate of HR is not. Therefore, these assays indicate that loss of Tpp1 affects the NHEJ pathway and loss of Mre11 affects the HR pathway. Therefore, the DSBs produced by bleomycin in the double mutant could not be repaired by either of the major DSB repair pathways resulting in SC.

4.4 The importance of resection in *tpp1Δ mre11Δ* SC interaction

Most of the SC interactions (ie. 4 out of 5 interactions) that I observed with *tpp1Δ* in the presence of bleomcyin were with genes implicated in the resection of DSBs. Previously it was

shown that *apn1Δ* and *apn2Δ,* which are also involved in resection, induced SC with *tpp1Δ* in the presence of bleomycin (Vance & Wilson, 2001). Further emphasizing the importance of DSB resection in these *tpp1* SC interactions, loss of *tpp1Δ* strongly suppressed the bleomycin sensitivity of *rad9* mutants. Rad9 inhibits resection; thus, its deletion promotes resection (Longhese at al., 2010). Finally, deletions of *RAD51*, *RAD52*, and *RAD50,* which are involved in HR but are not involved in resection, did not result in SC with *tpp1Δ* in the presence of bleomycin. All of these results support the hypothesis that DSB resection has an important role in the SC with *tpp1Δ* in the presence of bleomycin.

4.5 A hypothesis for the mechanism of *tpp1Δ mre11Δ* SC interaction

Bleomycin produces modified DSBs, which are unlike the DSBs generated by the activity of endonucleases such as the HO or ISceI endonucleases that generate "clean" DSBs that can be ligated without further processing. DSBs can be repaired by either NHEJ or HR. However, modified DSBs produced by bleomycin or ionizing radiation or oxidation must be converted to the free DSBs before the ligation steps of DNA repair pathways. In the HR pathway, the modified ends can be removed by Mre11 or other genes with resection capabilities in the HR pathway. However, the NHEJ pathway does not rely on resection so the modified ends must be converted to free ends before the initiation of NHEJ pathway. We hypothesize that Tpp1 converts the modified ends to clean ends by removing the 3' phosphate and any attached moieties such as damaged bases; the clean end is then a substrate for the classical NHEJ pathway. Therefore, the deletion of Tpp1 blocks the conversion of modified ends produced by bleomycin to free ends thereby inhibiting the classical NHEJ pathway, and if Mre11 is also non-functional, the modified DSB can not be resected and repaired by the HR pathway resulting in SC.

4.6 Phenotypic suppression (PS) of cytotoxicity

Out of 486 potential interactions, 19 cases showed PS interactions. PS interactions are important as they help us to understand the mechanism underlying the DNA damage induced cytotoxicity. For example, the PS interaction of *rad52Δ* sensitivity to bleomycin by the loss of *tpp1Δ* was likely the result of Tpp1 being needed for the removal of 3' phosphate. The presence of 3' phosphate promotes the resection activity of Mre11. The PS interaction of *rad52Δ tpp1Δ* under the application of bleomycin might be due to the presence of 3' phosphates allowing for Mre11 resection of the double strand breaks (DSBs) possibly through a poorly characterized repair mechanism called Microhomology-Mediated End Joining (MMEJ).

Just as SC interactions could be used to predict therapeutic interventions, PS interactions could suggest that certain therapies could be non-productive or even cause resistance to treatment. Resistance to chemotherapeutic agents is often produced by either bypassing pathway deficiencies or by re-modeling the DNA damage response (Bouwman & Jonkers, 2012). For example, platinum resistance responses might be caused by changes in nucleotide excision repair (NER) and mismatch repair (MMR) activity. Increased expression of ERCC1 in NER repair pathway can induce resistance to cisplatin (Martin, et al., 2008). Conversely, when MMR is deficient in cancer cells, the cells become resistant to platinum-based agents and can continue to proliferate (Martin et al., 2008).

4.7 Application of *TPP1* deletion or PNKP1 inhibition in cancer therapy

One of the important findings of my project is that Tpp1 is needed for NHEJ of modified DSBs. The only previous evidence that Tpp1 might have a role in NHEJ comes from a study of PNKP1, the human ortholog of Tpp1, that demonstrated PNKP interacts with the DNA repair scaffold XRCC4 to promote DSB ligation during NHEJ (Weinfeld et al., 2011). NHEJ plays a

critical role in the vertebrate immune system (Lieber, et al., 2004). However, the presence of Tpp1 is not important in this process since the DSB ends are clean and do not need further processing by PNKP before ligation. Therefore, PNKP inhibition could block NHEJ of DSBs induced by endogenous or exogenous DNA damage and induce SC in Mre11-deficient tumour cells without having any effect on normal cells or the immune system. Further supporting PNKP inhibition as a way to selectively target DNA damage induced DSBs, PNKP inhibition induces SL in *SHP1*-depleted cells. *SHP1* is a negative regulator of reactive oxygen species, and knocking down of *SHP1* increases the levels of reactive oxygen species (Mereniuk et al., 2012). Therefore, increasing the amount of free radicals by *SHP1* depletion induced more DNA damage with modified DSBs similar to those caused by bleomycin. These modified DSBs require processing by PNKP and as a result SC is induced in SHP1 depleted cells (Mereniuk et al., 2012).

The aim of this project was to identify SC interactions. Now that SC interactions have been identified, we can use large scale approaches such as Synthetic Genetic Array to extend from the small number of GIN genes tested to the entire GIN gene collection or even the entire gene knockout collection. We could also test other DNA repair enzymes for interactions to find interaction hubs that are highly connected with different DDAs. Finally these interactions can be tested for conservation in mammalian cell culture and could lead to new therapeutic approaches.

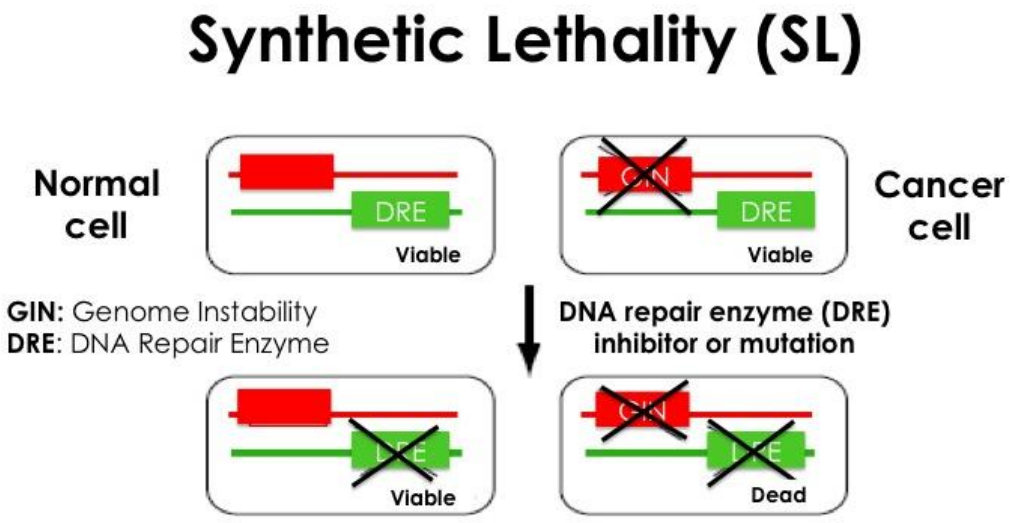

Figure 1: Synthetic Lethal (SL) interaction. Somatic mutations found in tumour cells can be leveraged for selective killing by inhibiting a second protein (DNA repair enzyme inhibitor) that is required for viability in the mutant cells but is not required in normal cells.

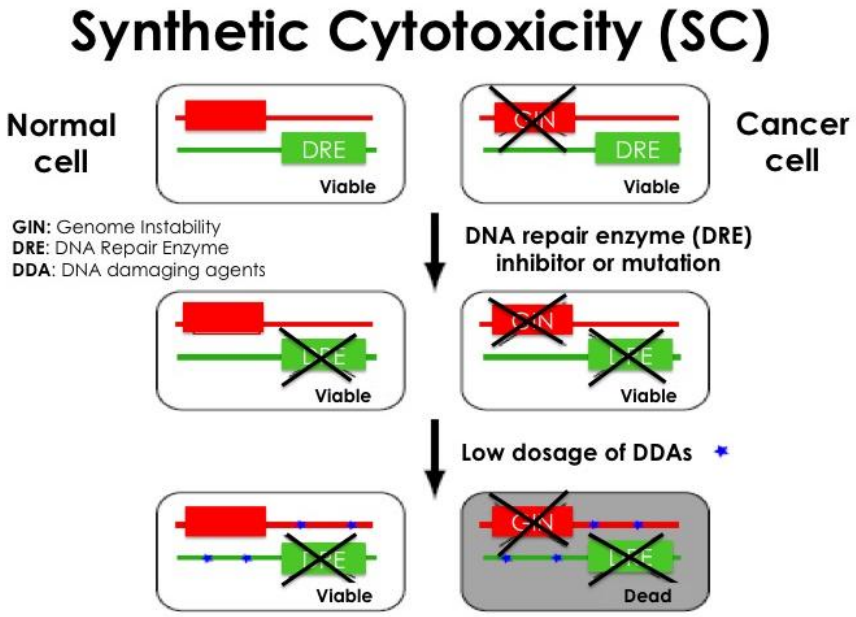

Figure 2: **Synthetic Cytotoxicity (SC) interaction**. In the cases that the combination of a somatic mutation and a DNA repair enzyme inhibitor does not result in synthetic lethality, the combination of a somatic mutation and a DNA repair enzyme inhibitor might sensitize the tumour cells to low dosage of a DNA damaging agent**.**

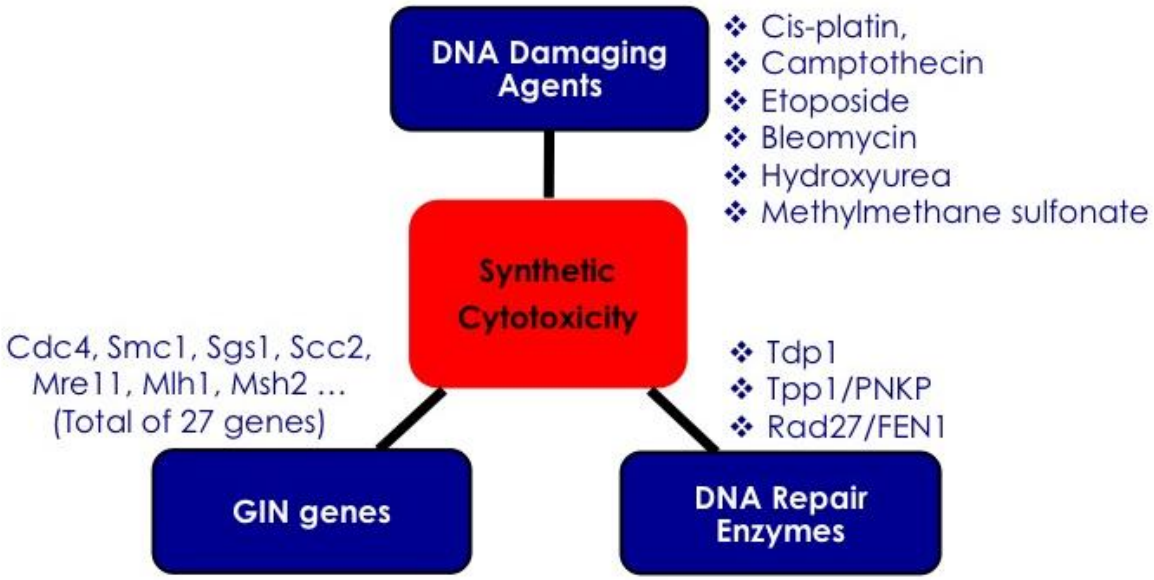

Figure 3: Three main components of SC interaction. To discover Synthetic Cytotoxic interactions, we need to identify GIN genes, DNA Repair Enzymes, and DNA Damaging Agents.

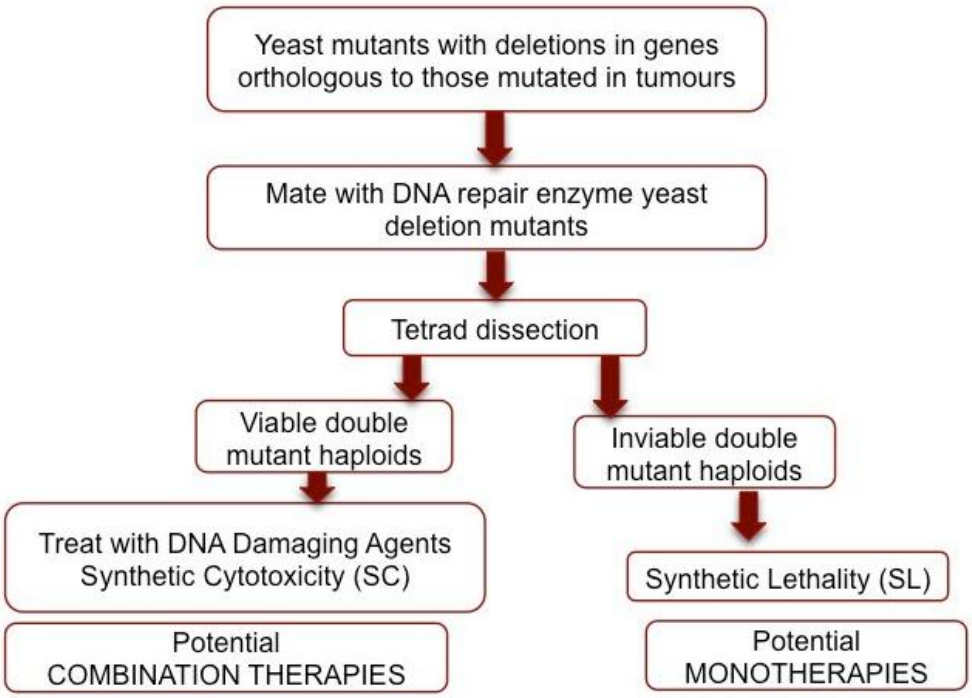

Figure 4: Procedure to obtain either viable or inviable double deleted haploids after tetrad dissection. Viable double mutants can be tested for SC under the application of low dosage of six DDAs (potential combination therapy), and inviable double mutants are good candidate for potential monotherapy.

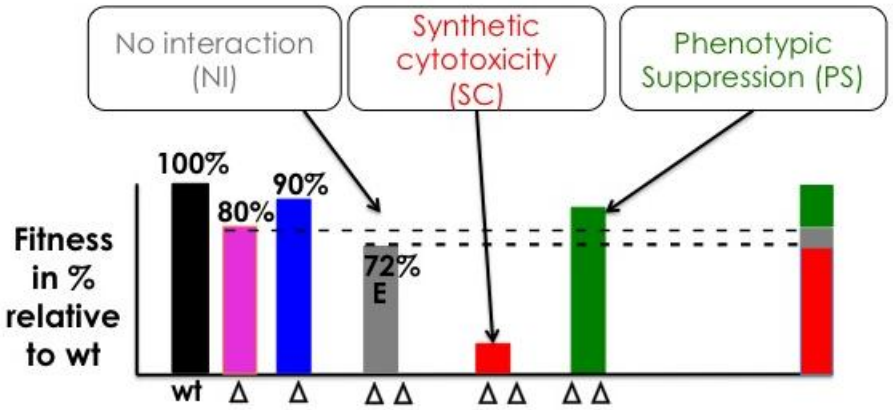

Figure 5: Possible Growth Curve outcomes in the presence of DDAs. No interaction (NI, grey), synthetic cytotoxicity (SC, red), phenotypic suppression (PS, green) are the main interactions that were identified.

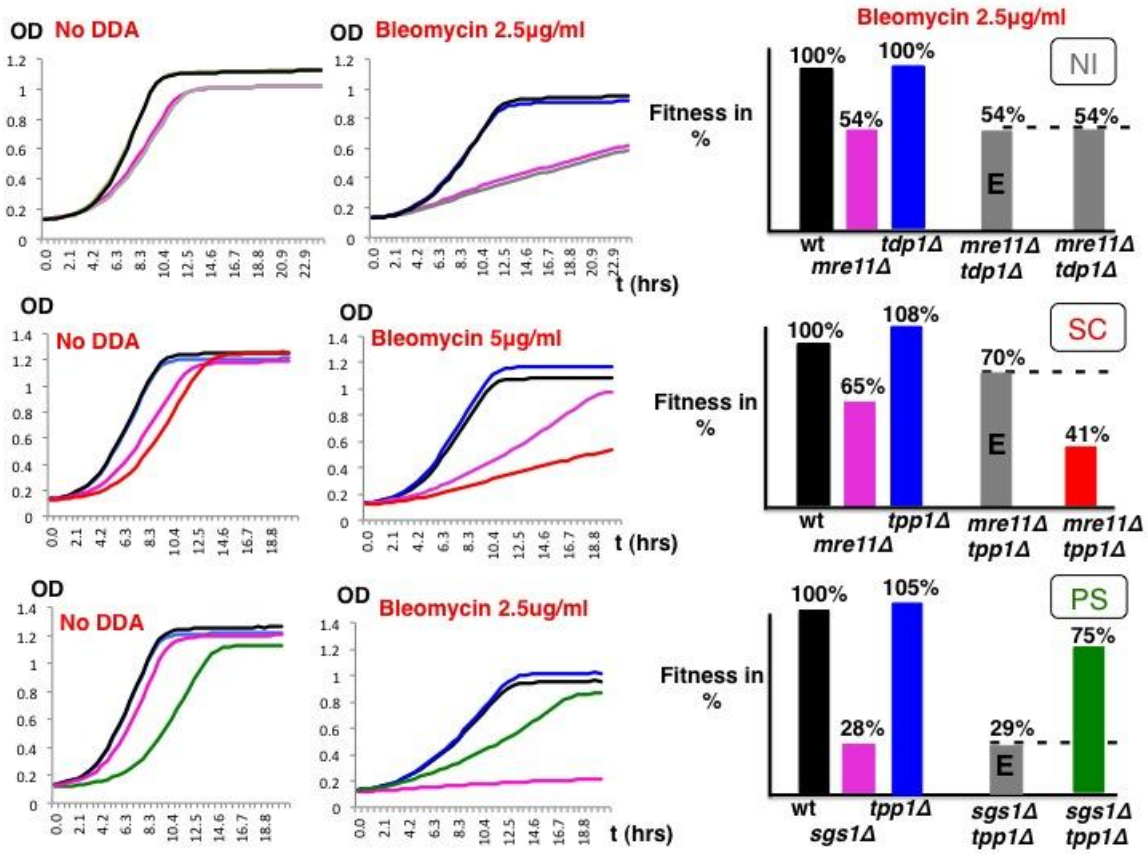

Figure 6: Examples of the three possible outcomes for growth curves in the presence of DDAs. A) *tdp1Δ mre11Δ* in the presence of 2.5μg/ml bleomycin is an example of No Interaction (NI). B) *tpp1Δ mre11Δ* in the presence of 2.5μg/ml bleomycin is an example of Synthetic Cytotoxicity (SC) interaction. C) *tpp1Δ sgs1Δ* in the presence of 2.5μg/ml bleomycin is an example of Phenotypic Suppression (PS).

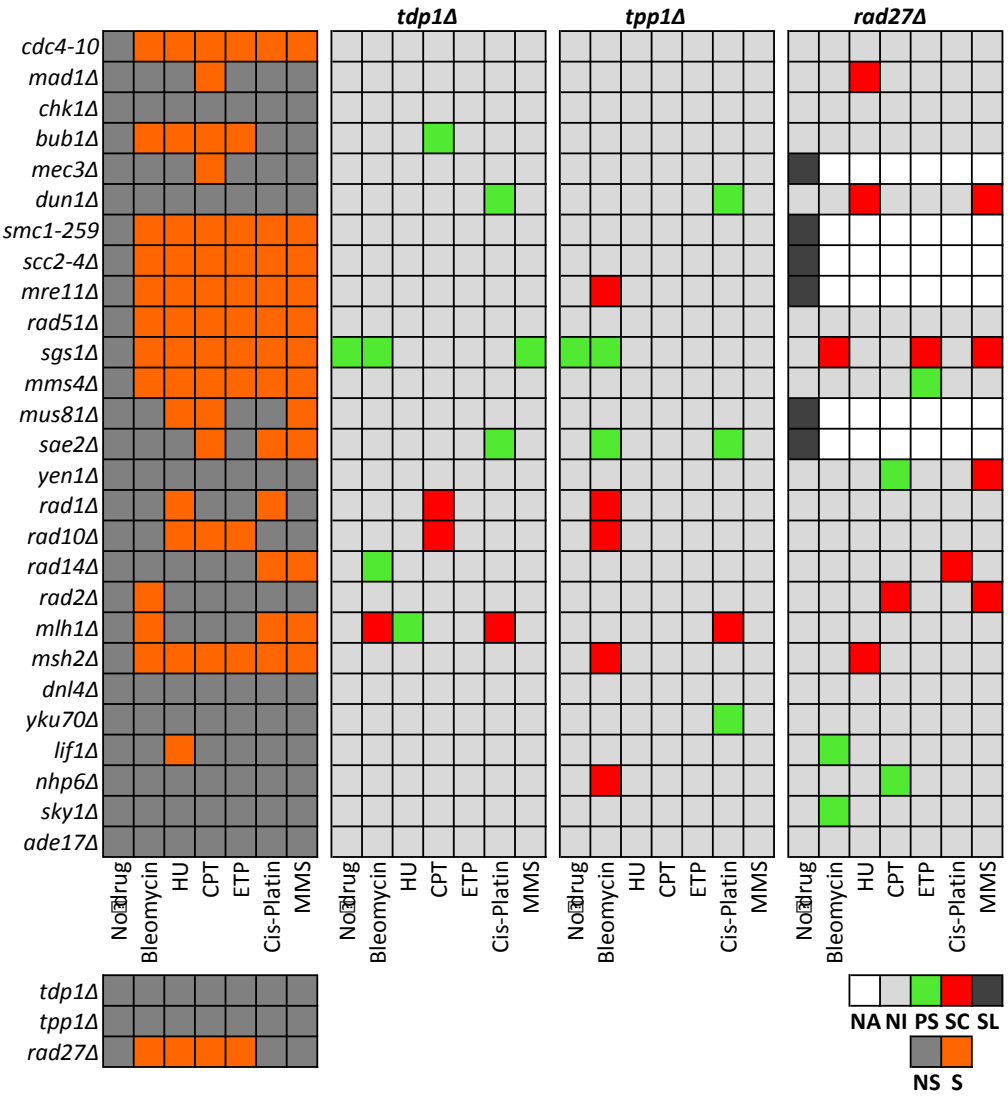

Figure 7: Summarizing of all the interactions. 81 haploid double mutants under the application of six different DDAs (486 combinations). Out of 486 potential interactions, 6 cases showed SL, 21 cases showed SC, and 19 cases showed phenotypic suppression. Not Applicable (NA, white), No Interaction (NI, grey), Phenotypic Suppression (PS, green), Synthetic Cytotoxicity (SC, red); sensitivity (S) and not sensitivity (NS) of single mutant in the presence of DDAs were presented by orange and dark grey colors respectively.

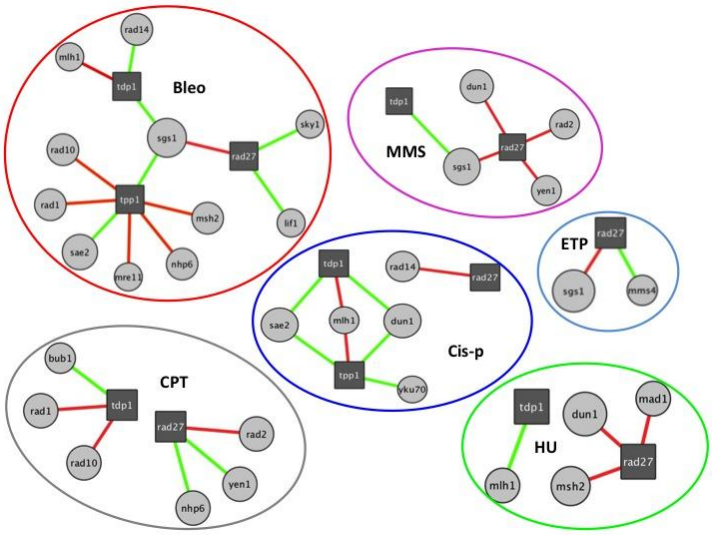

Figure 8: Interesting interactions categorized with six different DDAs. Red lines indicate SC interactions, and the green lines indicate PS interactions.

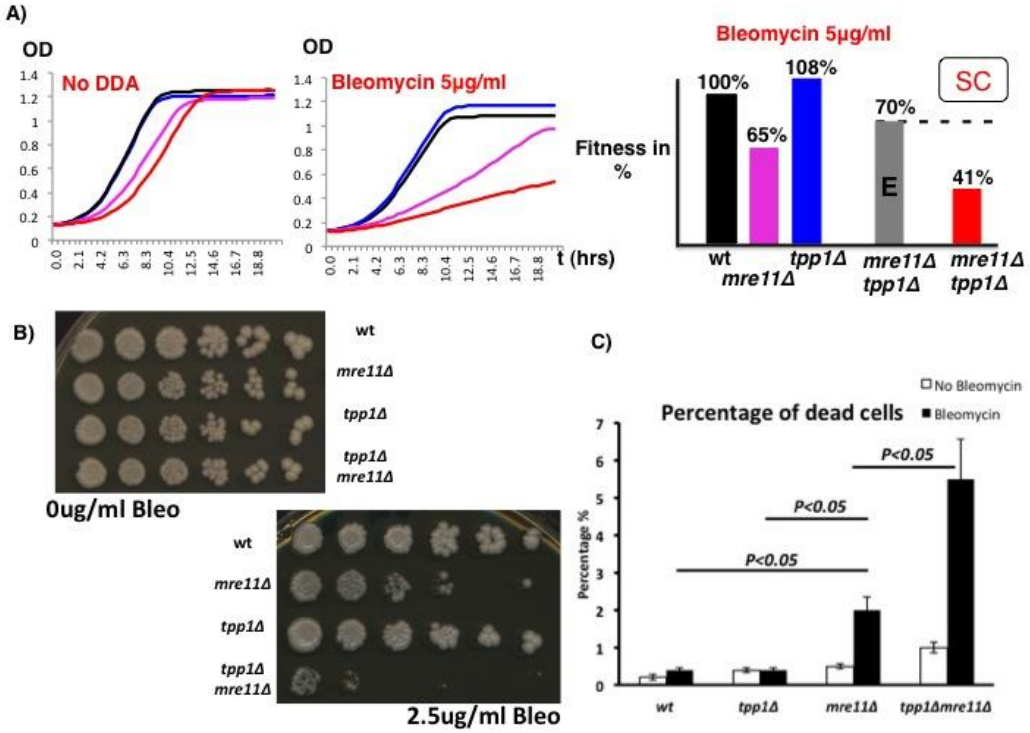

Figure 9: SC interaction of *tpp1Δ mre11Δ* in the presence of bleomycin. A) Growth curve and fitness percentage of wild type, *tpp1Δ*, *mre11Δ*, *tpp1Δ mre11Δ* in the presence of 2.5µg/ml bleomycin B) Spot assay of wt, *tpp1Δ*, *mre11Δ*, *tpp1Δ mre11Δ* in the presence and absence of 2.5µg/ml bleomycin C) Percentage of dead cells with no bleomycin and after application of 2.5µg/ml bleomycin for 3h for wt, *tpp1Δ*, *mre11Δ*, and *tpp1Δ mre11Δ*. Error bars are standard deviation. T-Test was used to calculate p-value.

A)

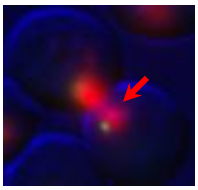

B)

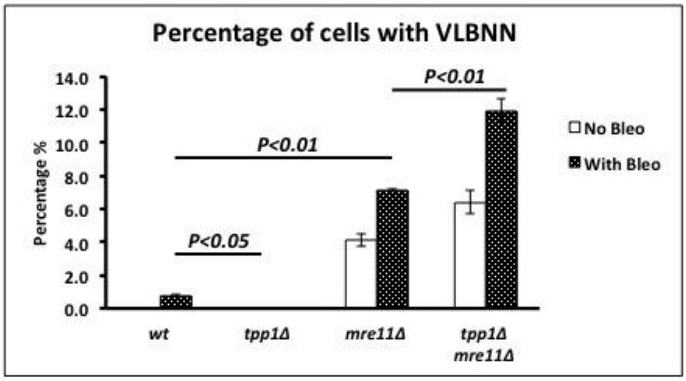

Figure 10: The percentage of cells with very large budded nucleus in the neck (VLBNN). A) A cell with VLBNN (red arrow) B) The percentage of the cells with VLBNN in wild type, *tpp1Δ*, *mre11Δ*, *tpp1Δ mre11Δ* in the presence and absence of bleomycin. Error bars are standard deviation. T-Test was used to calculate p-value.

A)

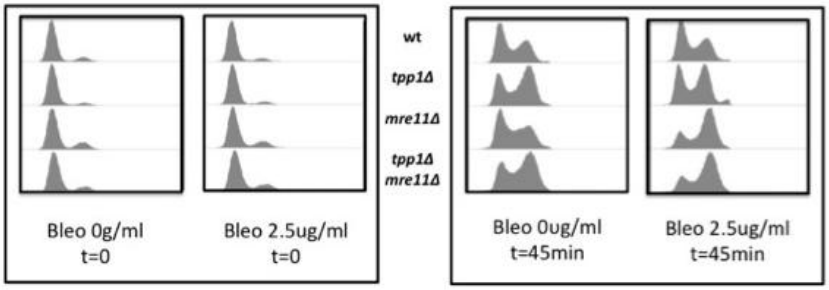

B)

DDAs	wt G1	wt G2/M	tppΔ G1	tppΔ G2/M	mre11Δ G1	me11Δ G2/M	tppΔmre11Δ G1	tppΔ me11Δ G2/M
No Bleo	75.1	24.0	80.7	19.3	59.7	40.8	39.7	53.8
Bleo	64.6	35.4	75.7	25.1	35.3	64.7	37.5	62.5

Figure 11: Examine the cell cycle arrest of *tpp1Δmre11Δ* in the presence and absence of bleomycin by Flow cytometry and cell counting. A) Flow Cytometry, the cells were arrested in G1 stage by alpha factor, and the cell cycle of wild type, *tpp1Δ*, *mre11Δ*, and *tpp1Δ mre11Δ* in the presence and absence of bleomycin were estimated after 45minutues. B) The number of cells in G1, G2/M stages were counted for wild type, *tpp1Δ*, *mre11Δ*, and *tpp1Δ mre11Δ* in the absence of bleomycin and after application of bleomycin for 3h.

A)

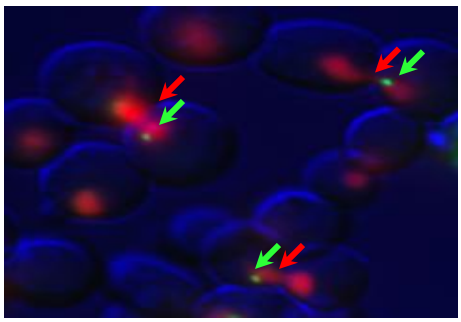

B)

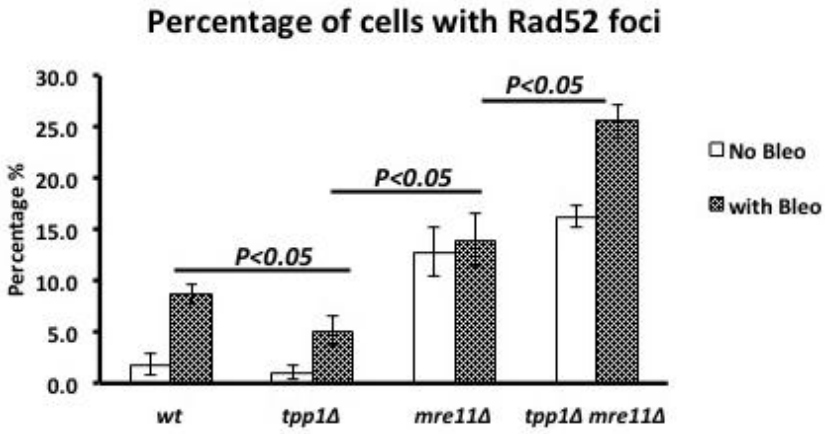

C)

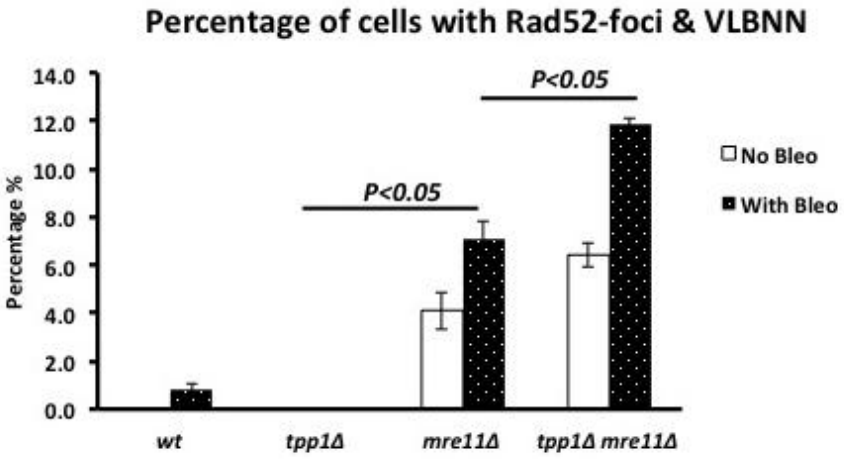

Figure 12: Estimate the percentage of cells with very large budded nucleolus in the neck (VLBNN) and Rad52-foci. A) Cell with VLBNN (red arrow) and Rad52 foci (green arrow), B) the percentage of the cells with Rad52 foci, C) the percentage of cells with both VLBNN and Rad52 foci. Error bars are standard deviation. T-Test was used to calculate p-value.

A)

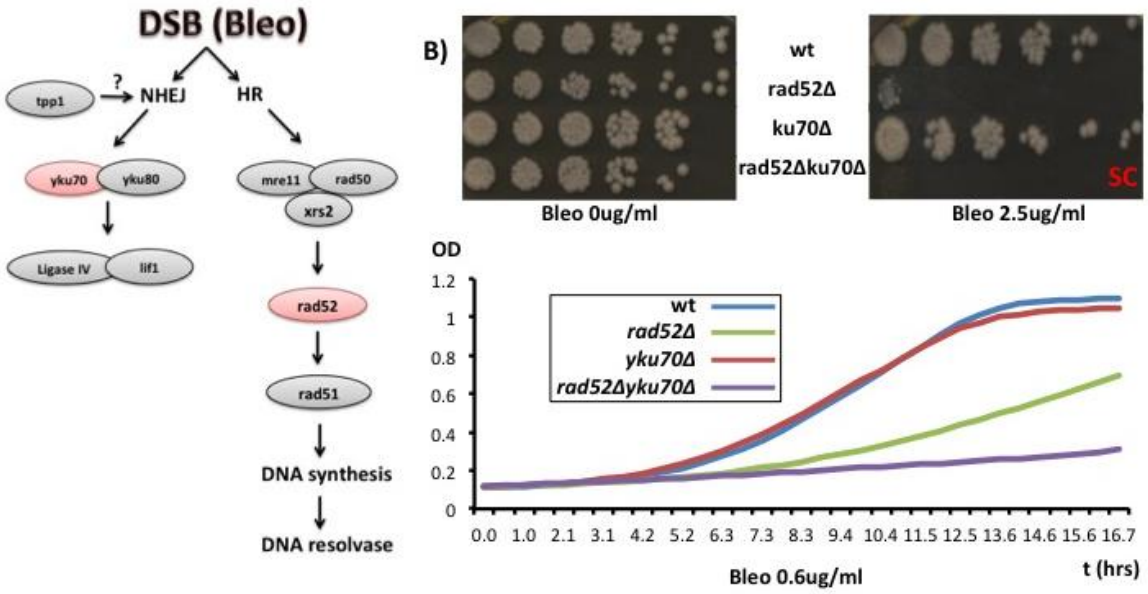

C)

Interactions	Types of Interactions	DNA repair pathway Δ
yku70Δ rad52Δ (Bleomycin)	SC	NHEJ, HR
yku70Δ mre11Δ (Bleomycin)	SC	NHEJ, MMEJ, HR
xrs2Δ tpp1Δ (Bleomycin)	SC	NHEJ, MMEJ, HR
yku70Δ tpp1Δ (Bleomycin)	NI	NHEJ
lif1Δ tpp1Δ (Bleomycin)	NI	NHEJ
dnl4Δ tpp1Δ (Bleomycin)	NI	NHEJ
rad51Δ tpp1Δ (Bleomycin)	NI*	HR, NHEJ
rad52Δ tpp1Δ (Bleomycin)	PS*	HR, NHEJ
mre11Δ rad52Δ (Bleomycin)	SC*	HR, MMEJ

Figure 13: Deletions of two main DNA repair pathways (HR & NHEJ) causes SC in the presence of bleomycin. (A&B) deletion of essential genes in two main double strand breaks (DSBs) DNA repair pathways (ie. HR & NHEJ) in the presence of bleomycin induce SC. (C) The results of deleted essential genes in two main DNA repair pathways in combination to *mre11Δ* and *tpp1Δ* deletion in the presence of bleomycin; refer to Table 5 for PS/SC calculations. Microhomology-mediated end joining (MMEJ).

A)

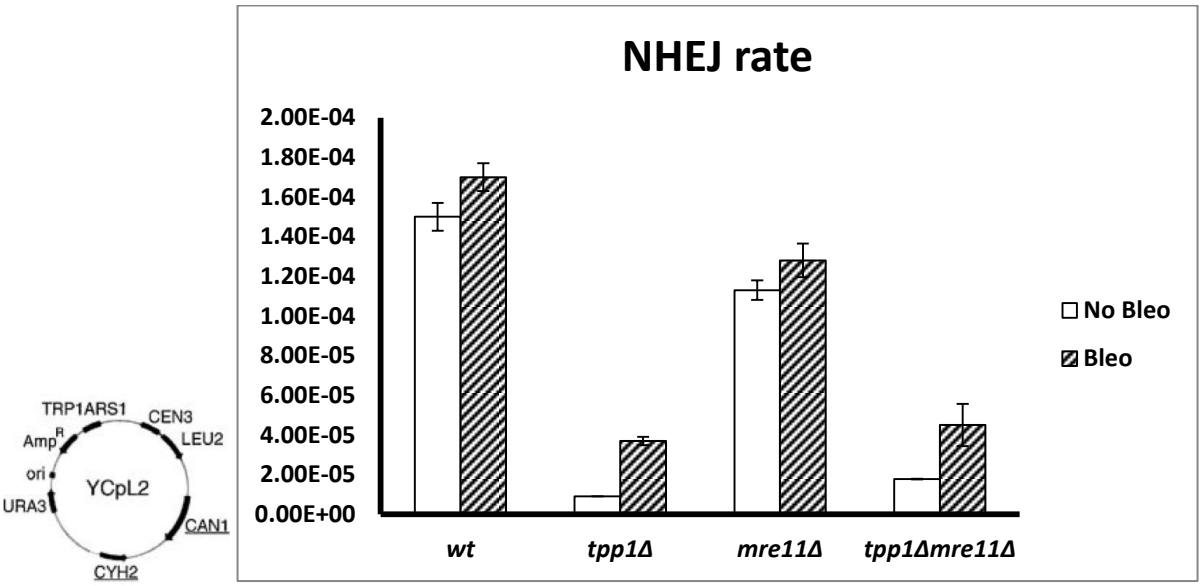

B)

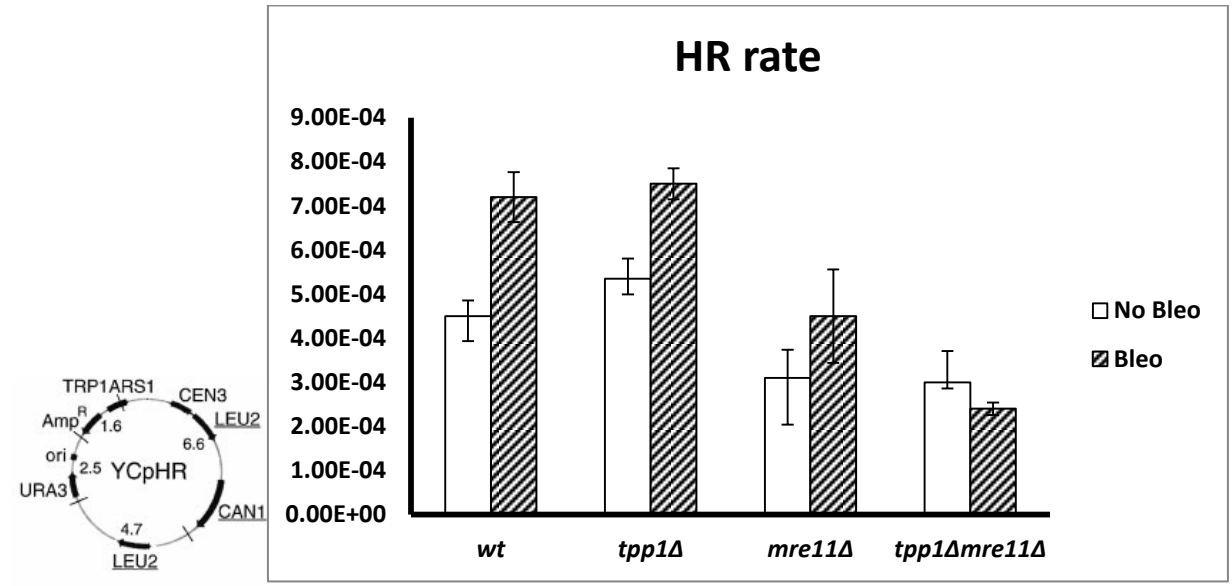

Figure 14: HR and NHEJ frequencies of wt, *tpp1Δ*, *mre11Δ*, *tpp1Δ mre11Δ* in the presence and absence of bleomycin. A) YCLP2 plasmid and NHEJ frequencies; simultaneous loss of the CAN1 and CYH2 genes can be identified by the growth of colonies on Canavanine and Cycloheximide containing plates**.** B) YCpHR plasmid and HR plasmids; loss of CAN1 gene can be identified by the growth of colonies on Canavanine plates. Error bars are standard deviation.

Strains	Genotype
YNM 3	*tdp1Δ::KanMx, his3Δ1, leu2Δ0, ura3Δ0, lys2Δ0*
YNM 7	*rad27Δ::HyMx, his3Δ1, leu2Δ0, ura3Δ0, lys2Δ0*
YNM 5	*tpp1Δ::KanMx, his3Δ1, leu2Δ0, ura3Δ0, lys2Δ0*
YNM 13	*tpp1Δ::KanMx, his3Δ1, leu2Δ0, ura3Δ0, lys2Δ0*
YNM 34	*dun1Δ::KanMx, his3Δ1, leu2Δ0, ura3Δ0, lys2Δ0*
YNM 40	*yen1Δ::KanMx, his3Δ1, leu2Δ0, ura3Δ0, lys2Δ0*
YNM 76	*rad1Δ::URA3, his3Δ1, leu2Δ0, ura3Δ0, lyp1Δ, met15Δ0, can1Δ::STE2pr-his5+*
YNM 77	*rad51Δ::URA3, his3Δ1, leu2Δ0, ura3Δ0, lyp1Δ, met15Δ0, can1Δ::STE2pr-his5+*
YNM 75	*sgs1Δ::URA3, his3Δ1, leu2Δ0, ura3Δ0, lyp1Δ, met15Δ0, can1Δ::STE2pr-his5+*
YNM 78	*mad1Δ::URA3, his3Δ1, leu2Δ0, ura3Δ0, met15Δ0, lyp1Δ, can1Δ::STE2pr-his5+*
YNM 80	*cdc4-10::URA3, his3Δ1, leu2Δ0, ura3Δ0, lys2Δ0 or LYS2, met15Δ0 or MET15, LYP1, can1Δ::LEU2-MFA1pr::HIS3*
YNM 81	*mre11Δ::NatMx, his3Δ1, leu2Δ0, ura3Δ0, lyp1Δ, met15Δ0, can1Δ::STE2pr-his5+*
YNM 82	*smc1-259::URA3, his3Δ1, leu2Δ0, ura3Δ0, lys2Δ0 or LYS2, met15Δ0 or MET15, LYP1, can1Δ::LEU2-MFA1pr::HIS3*
YNM 83	*scc2-4::URA3, his3Δ1, leu2Δ0, ura3Δ0, lys2Δ0 or LYS2, met15Δ0 or MET15, LYP1, can1Δ::LEU2-MFA1pr::HIS3*
YNM 137	*rad2Δ::KanMx, his3Δ1, leu2Δ0, ura3Δ0, lys2Δ0*
YNM 138	*nhp6Δ::KanMx, his3Δ1, leu2Δ0, ura3Δ0, lys2Δ0*
YNM 139	*rad14Δ::KanMx, his3Δ1, leu2Δ0, ura3Δ0, lys2Δ0*
YNM 142	*sae2Δ::KanMx, his3Δ1, leu2Δ0, ura3Δ0, lys2Δ0*
YNM 143	*mec3Δ::KanMx, his3Δ1, leu2Δ0, ura3Δ0, lys2Δ0*
YNM 144	*bub1Δ::KanMx, his3Δ1, leu2Δ0, ura3Δ0, lys2Δ0*
YNM 146	*msh2Δ::KanMx, his3Δ1, leu2Δ0, ura3Δ0, lys2Δ0*
YNM 147	*rad10Δ::KanMx, his3Δ1, leu2Δ0, ura3Δ0, lys2Δ0*
YNM 148	*sky1Δ::KanMx, his3Δ1, leu2Δ0, ura3Δ0, lys2Δ0*
YNM 150	*dnl4Δ::KanMx, his3Δ1, leu2Δ0, ura3Δ0, lys2Δ0*
YNM 155	*mlh1Δ::KanMx, his3Δ1, leu2Δ0, ura3Δ0, lys2Δ0*
YNM 161	*tdp1Δ::NatMx, his3Δ1, leu2Δ0, ura3Δ0, lys2Δ0*
YNM 164	*tpp1Δ::NatMx, his3Δ1, leu2Δ0, ura3Δ0, lys2Δ0*
YNM 216	*chk1Δ::KanMx, his3Δ1, leu2Δ0, ura3Δ0, lys2Δ0*
YNM 217	*mms4Δ::KanMx, his3Δ1, leu2Δ0, ura3Δ0, lys2Δ0*
YNM 218	*yku70Δ::KanMx, his3Δ1, leu2Δ0, ura3Δ0, lys2Δ0*
YNM 219	*lif1Δ::KanMx, his3Δ1, leu2Δ0, ura3Δ0, lys2Δ0*
YNM 220	*mus81Δ::KanMx, his3Δ1, leu2Δ0, ura3Δ0, lys2Δ0*
YNM 225	*ade17Δ::KanMx, his3Δ1, leu2Δ0, ura3Δ0, lys2Δ0*
YNM 360	*mre11Δ::KanMx, his3Δ1, leu2Δ0, ura3Δ0, lys2Δ0*
YNM 373	*rad52-GFP::HIS, Hta2-mchery::HPH, his3Δ1, leu2Δ0, ura3Δ0*

Table 1: The list of *S. cerevisiae* single deleted strains. The strains that applied for growth curve, spot assay and microscopy analysis; all the strains are *MAT-α*, except YNM3, YNM7, YNM13, YNM161, YNM164, YNM 360, and YNM373, which are *MAT-a*.

Strains	Genotype	Strains	Genotype	Strains	Genotype
YNM101	YNM161 YNM34	**YNM103**	YNM7 YNM34	**YNM216**	YNM164 YNM34
YNM278	YNM161 YNM40	**YNM286**	YNM7 YNM40	**YNM282**	YNM164 YNM40
YNM43	YNM3 YNM76	**YNM65**	YNM7 YNM76	**YNM48**	YNM13 YNM76
YNM60	YNM3 YNM77	**YNM61**	YNM7 YNM77	**YNM62**	YNM13 YNM77
YNM38	YNM3 YNM75	**YNM68**	YNM7 YNM75	**YNM99**	YNM13 YNM75
YNM37	YNM3 YNM78	**YNM59**	YNM7 YNM78	**YNM51**	YNM13 YNM78
YNM54	YNM3 YNM80	**YNM72**	YNM7 YNM80	**YNM52**	YNM13 YNM80
YNM45	YNM3 YNM81	**YNM57**	YNM7 YNM81	**YNM280**	YNM164 YNM137
YNM53	YNM3 YNM82	**YNM58**	YNM13 YNM81	**YNM199**	YNM164 YNM138
YNM46	YNM3 YNM83	**YNM54**	YNM7 YNM82	**YNM200**	YNM164 YNM139
YNM284	YNM161 YNM137	**YNM63**	YNM7 YNM83	**YNM190**	YNM164 YNM144
YNM189	YNM161 YNM138	**YNM272**	YNM7 YNM137	**YNM192**	YNM164 YNM146
YNM177	YNM161 YNM139	**YNM180**	YNM7 YNM138	**YNM232**	YNM164 YNM147
YNM184	YNM161 YNM142	**YNM174**	YNM7 YNM139	**YNM230**	YNM164 YNM148
YNM182	YNM161 YNM143	**YNM178**	YNM7 YNM142	**YNM254**	YNM164 YNM150
YNM173	YNM161 YNM144	**YNM187**	YNM7 YNM143	**YNM69**	YNM164 YNM155
YNM195	YNM161 YNM146	**YNM170**	YNM7 YNM144	**YNM204**	YNM164 YNM216
YNM210	YNM161 YNM147	**YNM196**	YNM7 YNM146	**YNM234**	YNM164 YNM217
YNM240	YNM161 YNM148	**YNM258**	YNM7 YNM147	**YNM208**	YNM164 YNM218
YNM202	YNM161 YNM150	**YNM226**	YNM7 YNM148	**YNM250**	YNM164 YNM219
YNM167	YNM161 YNM155	**YNM256**	YNM7 YNM150	**YNM190**	YNM164 YNM144
YNM267	YNM161 YNM216	**YNM191**	YNM7 YNM155	**YNM192**	YNM164 YNM146
YNM212	YNM161 YNM217	**YNM265**	YNM7 YNM216	**YNM232**	YNM164 YNM147
YNM276	YNM161 YNM218	**YNM206**	YNM7 YNM217	**YNM269**	YNM164 YNM225
YNM242	YNM161 YNM219	**YNM274**	YNM7 YNM218	**YNM410**	BY4742 YNM373
YNM260	YNM161 YNM220	**YNM252**	YNM7 YNM219	**YNM409**	YNM5 YNM373
YNM238	YNM161 YNM225	**YNM262**	YNM7 YNM220	**YNM408**	YNM81 YNM373
YNM383	YNM57 YNM373	**YNM271**	YNM7 YNM225		

Table 2: The list of *S. cerevisiae* double deleted strains. The strains that applied for growth curve, spot assay and microscopy analysis; all the strains are *MAT-*α, except for YNM58, which is mat-a. BY4741, and BY4742 were used as wild type strains.

S. cerevisiae Gene name (ORF)	Function	*H. sapiens* gene symbol	CIN phenotype	Mutator Phenotype	Cancer Census
CDC4 (YFL009W)	Cell cycle checkpoints	FBXW7	Yes		Yes
MAD1 (YGL086W)	Cell cycle checkpoints	MAD1L1	Yes		No
CHK1 (YBR274W)	Cell cycle checkpoints	CHEK1	Yes	Yes	No
BUB1 (YGR188C)	Cell cycle checkpoint	BUB1	Yes		No
MEC3 (YLR288C)	Cell cycle checkpoints	HUS1			No
DUN1 (YDL101C)	Cell cycle checkpoints	CHEK2	Yes	Yes	Yes
SMC1 (YFL008W)	Sister Chromatid Cohesions	SMC1A	Yes		No
SCC2 (YDR180W)	Sister Chromatid Cohesions	RAD21	Yes		No
MRE11 (YMR224C)	Nuclease activity	MRE11A	Yes	Yes	No
RAD51 (YER095W)	Homologous Recombination (HR)	RAD51	Yes	Yes	Yes
SGS1 (YMR190C)	Helicases	BLM	Yes	Yes	Yes
MMS4 (YBR098W)	Nuclease activity	EME1			No
MUS81 (YDR386W)	Nuclease activity	MUS81	Yes		No
SAE2 (YGL175C)	Nuclease activity	SAE2			No
YEN1 (YER041W)	Resolvase	GEN1			No
RAD1 (YPL022W)	Nuclease activity	ERCC4	Yes	Yes	Yes
RAD10 (YML095C)	Nuclease activity	ERCC1	Yes	Yes	No
RAD14 (YMR201C)	Nucleotide excision repair pathway	XPA			Yes
RAD2 (YGR258C)	Nuclease activity	RAD2		Yes	No
MLH1 (YMR167W)	Mismatch repair (MMR)	MLH1		Yes	Yes
MSH2 (YOL090W)	Mismatch repair (MMR)	MSH2		Yes	Yes
DNL4 (YOR005C)	DNA ligase	LIG4		Yes	No
YKU70 (YMR284W)	Non-homologous end joining (NHEJ)	KU70			No
LIF1 (YGL090W)	DNA ligase	XRCC4			No
NHP6 (YPR052C)	Nucleosomes remodeling	ATIC	Yes		No
SKY1 (YMR216C)	SR protein kinases	SRPK1			No
ADE17 (YMR120C)	Enzyme of purine biosynthesis	ATIC	Yes		No

Table 3: The list of 27 GIN genes in yeast. The function of each gene, and their orthologs in human, their mutation and/or CIN phenotypes, and their existence in Cancer Census were indicated in this Table.

Interactions	Fitness%	SD	DDA [concentration]
wild type	100	0	Bleomycin [2.5µg/ml]
tpp1Δ	108.27	2.77	Bleomycin [2.5µg/ml]
mre11Δ	64.73	0.62	Bleomycin [2.5µg/ml]
***mre11Δ tpp1Δ* (Obsv.)**	41.34	1.22	Bleomycin [2.5µg/ml]
***mre11Δ tpp1Δ* (Exp.)**	70.08	1.85	Bleomycin [2.5µg/ml]
wild type	100	0	Bleomycin [2.5µg/ml]
tpp1Δ	93.83	2.45	Bleomycin [2.5µg/ml]
msh2Δ	82.23	2.57	Bleomycin [2.5µg/ml]
***msh2Δ tpp1Δ* (Obsv.)**	59.61	1.84	Bleomycin [2.5µg/ml]
***msh2Δ tpp1Δ* (Exp.)**	77.20	4.44	Bleomycin [2.5µg/ml]
wild type	100	0	Bleomycin [2.5µg/ml]
tpp1Δ	103.90	2.66	Bleomycin [2.5µg/ml]
rad10Δ	110.62	3.18	Bleomycin [2.5µg/ml]
***rad10Δ tpp1Δ* (Obsv.)**	80.32	1.30	Bleomycin [2.5µg/ml]
***rad10Δ tpp1Δ* (Exp.)**	114.88	0.94	Bleomycin [2.5µg/ml]
wild type	100	0	Bleomycin [2.5µg/ml]
tpp1Δ	94.80	3.72	Bleomycin [2.5µg/ml]
rad1Δ	96.34	4.67	Bleomycin [2.5µg/ml]
***rad1Δ tpp1Δ* (Obsv.)**	81.07	1.22	Bleomycin [2.5µg/ml]
***rad1Δ tpp1* (Exp.)**	91.423	7.85	Bleomycin [2.5µg/ml]
wild type	100	0	Bleomycin [2.5µg/ml]
tdp1Δ	113.12	2.30	Bleomycin [2.5µg/ml]
mlh1Δ	85.08	4.81	Bleomycin [2.5µg/ml]
***mlh1Δ tdp1Δ* (Obsv.)**	35.15	0.54	Bleomycin [2.5µg/ml]
***mlh1Δ tdp1Δ* (Exp.)**	96.31	7.22	Bleomycin [2.5µg/ml]
wild type	100	0	Bleomycin [2.5µg/ml]
tpp1Δ	104.39	0.37	Bleomycin [2.5µg/ml]
nhp6Δ	81.49	0.68	Bleomycin [2.5µg/ml]
***nhp6Δ tpp1Δ* (Obsv.)**	49.97	0.42	Bleomycin [2.5µg/ml]
***nhp6Δ tpp1Δ* (Exp.)**	85.07	0.74	Bleomycin [2.5µg/ml]
wild type	100	0	Bleomycin [1.25µg/ml]
rad27Δ	93.62	1.27	Bleomycin [1.25µg/ml]
sgs1Δ	81.57	2.44	Bleomycin [1.25µg/ml]
***sgs1Δ rad27Δ* (Obsv.)**	40.57	4.39	Bleomycin [1.25µg/ml]
***sgs1Δ rad27Δ* (Exp.)**	76.38	3.24	Bleomycin [1.25µg/ml]
wild type	100	0	Etoposide [2mM]
rad27Δ	92.91	1.92	Etoposide [2mM]
sgs1Δ	94.61	6.11	Etoposide [2mM]
***sgs1Δ rad27Δ* (Obsv.)**	66.86	5.31	Etoposide [2mM]
***sgs1Δ rad27Δ* (Exp.)**	87.84	4.42	Etoposide [2mM]
wild type	100	0	Hydroxyurea [200mM]
mad1Δ	93.23	3.38	Hydroxyurea [200mM]
rad27Δ	110.64	4.99	Hydroxyurea [200mM]
***mad1Δ rad27Δ* (Obsv.)**	68.55	2.16	Hydroxyurea [200mM]
***mad1Δ rad27Δ* (Exp.)**	103.14	5.40	Hydroxyurea [200mM]
wild type	100	0	Hydroxyurea [200mM]
dun1Δ	111.03	8.65	Hydroxyurea [200mM]
rad27Δ	99.514	2.48	Hydroxyurea [200mM]
***dun1Δ rad27Δ* (Obsv.)**	50.11	2.00	Hydroxyurea [200mM]
***dun1Δ rad27Δ* (Exp.)**	110.63	11.26	Hydroxyurea [200mM]
wild type	100	0	Hydroxyurea [200mM]
rad27Δ	88.14	1.24	Hydroxyurea [200mM]
msh2Δ	77.13	3.01	Hydroxyurea [200mM]
***msh2Δ rad27Δ* (Obsv.)**	49.16	1.38	Hydroxyurea [200mM]
***msh2Δ rad27Δ* (Exp.)**	67.99	3.31	Hydroxyurea [200mM]

Interactions	Fitness%	SD	DDA [concentration]
wild type	100	0	MMS [0.01%]
rad27Δ	102.54	19.44	MMS [0.01%]
rad2Δ	65.24	2.67	MMS [0.01%]
***rad2Δ rad27Δ* (Obsv.)**	50.27	3.32	MMS [0.01%]
***rad2Δ rad27Δ* (Exp.)**	67.07	14.26	MMS [0.01%]
wild type	100	0	MMS [0.01%]
rad27Δ	111.47	1.65	MMS [0.01%]
sgs1Δ	108.58	4.17	MMS [0.01%]
***sgs1Δ rad27Δ* (Obsev.)**	47.04	2.00	MMS [0.01%]
***sgs1Δ rad27Δ* (Exp.)**	121.07	6.28	MMS [0.01%]
wild type	100	6.10	MMS [0.01%]
rad27Δ	99.49	0.89	MMS [0.01%]
yen1Δ	94.83	7.90	MMS [0.01%]
***yen1Δ rad27Δ* (Obsv.)**	56.61	4.81	MMS [0.01%]
***yen1Δ rad27Δ* (Exp.)**	94.32	7.44	MMS [0.01%]
wild type	100	0	MMS [0.01%]
dun1Δ	120.12	8.44	MMS [0.01%]
rad27Δ	114.20	7.64	MMS [0.01%]
***dun1 Δ rad27Δ* (Obsv.)**	68.13	3.80	MMS [0.01%]
***dun1 Δ rad27Δ* (Exp.)**	137.21	13.71	MMS [0.01%]
wild type	100	0	Camptothecin [25μM]
rad27Δ	83.79	0.65	Camptothecin [25μM]
rad2Δ	76.22	1.50	Camptothecin [25μM]
***rad2Δ rad27Δ* (Obsv.)**	56.42	0.60	Camptothecin [25μM]
***rad2Δ rad27Δ* (Exp.)**	63.87	1.29	Camptothecin [25μM]
wild type	100	0	Camptothecin [50μM]
tdp1Δ	102.34	9.87	Camptothecin [50μM]
rad1Δ	102.36	2.75	Camptothecin [50μM]
***rad1Δ tdp1Δ* (Obsv.)**	61.46	1.82	Camptothecin [50μM]
***rad1Δ tdp1Δ* (Exp.)**	104.92	12.91	Camptothecin [50μM]
wild type	100	0	Camptothecin [50μM]
tdp1Δ	98.48	4.58	Camptothecin [50μM]
rad10Δ	98.73	2.56	Camptothecin [50μM]
***rad10 Δ tdp1Δ* (Obsv.)**	59.42	2.28	Camptothecin [50μM]
***rad10Δ tdp1 Δ* (Exp.)**	97.28	6.52	Camptothecin [50μM]
wild type	100	0	Cis-Platin [1.2mM]
rad27Δ	115.32	0.75	Cis-Platin [1.2mM]
rad14Δ	122.54	1.79	Cis-Platin [1.2mM]
***rad14 Δ rad27Δ* (Obsv.)**	61.67	2.06	Cis-Platin [1.2mM]
***rad14 Δ rad27Δ* (Exp.)**	141.33	2.96	Cis-Platin [1.2mM]
wild type	100	0	Cis-Platin [1.4mM]
tdp1Δ	112.08	2.06	Cis-Platin [1.4mM]
mlh1Δ	90.01	1.92	Cis-Platin [1.4mM]
***mlh1Δ tdp1Δ* (Obsv.)**	70.55	2.98	Cis-Platin [1.4mM]
***mlh1Δ tdp1Δ* (Exp.)**	100.89	2.86	Cis-Platin [1.4mM]
wild type	100	0	Cis-Platin [1.4mM]
tpp1Δ	108.79	1.69	Cis-Platin [1.4mM]
mlh1Δ	68.90	4.12	Cis-Platin [1.4mM]
***mlh1Δ tpp1Δ* (Obsv.)**	31.47	0.91	Cis-Platin [1.4mM]
***mlh1 Δ tpp1Δ* (Exp.)**	74.96	4.69	Cis-Platin [1.4mM]

Table 4: Fitness calculations relative to wild type to identify SC interactions by using the area under the curve. The calculation of expected and observed fitness for 21 SC interactions under the application of different DDAs.

Interactions	Fitness%	SD	DDA [concentration]
wild type	100.00	0.00	NO DDA
tdp1Δ	96.10	1.67	NO DDA
sgs1Δ	54.91	1.24	NO DDA
***sgs1Δ tdp1Δ* (Obsv.)**	73.78	0.80	NO DDA
***sgs1Δ tdp1Δ* (Exp.)**	52.78	1.71	NO DDA
wild type	100.00	0.00	NO DDA
tpp1Δ	77.02	3.17	NO DDA
sgs1Δ	47.39	2.10	NO DDA
***sgs1Δ tpp1Δ* (Obsv.)**	82.70	3.75	NO DDA
***sgs1Δ tpp1Δ* (Exp.)**	36.53	2.92	NO DDA
wild type	100.00	0.00	Bleomycin [2.5µg/ml]
tdp1Δ	107.62	1.99	Bleomycin [2.5µg/ml]
rad14Δ	81.84	7.26	Bleomycin [2.5µg/ml]
***rad14Δ tdp1Δ* (Obsv.)**	113.82	0.68	Bleomycin [2.5µg/ml]
***rad14Δ tdp1Δ* (Exp.)**	88.10	8.32	Bleomycin [2.5µg/ml]
wild type	100.00	0.00	Bleomycin [2.5µg/ml]
tpp1Δ	114.12	1.07	Bleomycin [2.5µg/ml]
sae2Δ	85.32	1.23	Bleomycin [2.5µg/ml]
***sae2Δ tpp1Δ* (Obsv.)**	123.08	0.75	Bleomycin [2.5µg/ml]
***sae2Δ tpp1Δ* (Exp.)**	97.36	1.15	Bleomycin [2.5µg/ml]
wild type	100.00	0.00	Bleomycin [2.5µg/ml]
tdp1Δ	94.00	3.84	Bleomycin [2.5µg/ml]
sgs1Δ	41.39	1.22	Bleomycin [2.5µg/ml]
***sgs1Δ tdp1Δ* (Obsv.)**	68.24	3.36	Bleomycin [2.5µg/ml]
***sgs1Δ tdp1Δ* (Exp.)**	38.92	2.45	Bleomycin [2.5µg/ml]
wild type	100.00	0.00	Bleomycin [2.5µg/ml]
tpp1Δ	105.43	6.19	Bleomycin [2.5µg/ml]
sgs1Δ	27.74	1.33	Bleomycin [2.5µg/ml]
***sgs1Δ tpp1Δ* (Obsv.)**	74.64	5.37	Bleomycin [2.5µg/ml]
***sgsΔ tpp1* (Exp.)**	29.30	3.00	Bleomycin [2.5µg/ml]
wild type	100.00	0.00	Bleomycin [1.25µg/ml]
rad27Δ	74.76	4.42	Bleomycin [1.25µg/ml]
lif1Δ	109.19	3.60	Bleomycin [1.25µg/ml]
***lif1Δ rad27Δ* (Obsv.)**	96.10	1.38	Bleomycin [1.25µg/ml]
***lif1Δ rad27Δ* (Exp.)**	81.74	7.47	Bleomycin [1.25µg/ml]
wild type	100.00	0.00	Bleomycin [1.25µg/ml]
rad27Δ	92.31	3.28	Bleomycin [1.25µg/ml]
sky1Δ	120.09	2.22	Bleomycin [1.25µg/ml]
***sky1Δ rad27Δ* (Obsv.)**	111.25	0.07	Bleomycin [1.25µg/ml]
***sky1Δ rad27Δ* (Exp.)**	110.84	0.74	Bleomycin [1.25.µg/ml]
wild type	100.00	0.00	Hydroxyurea [200mM]
tdp1Δ	96.10	1.67	Hydroxyurea [200mM]
mlh1Δ	54.91	1.24	Hydroxyurea [200mM]
***mlh1Δ tdp1Δ* (Obsv.)**	73.78	0.80	Hydroxyurea [200mM]
***mlh1Δ tdp1Δ* (Exp.)**	52.78	1.71	Hydroxyurea [200mM]
wild type	100.00	0.00	MMS [0.01%]
tdp1Δ	96.25	2.47	MMS [0.01%]
sgs1Δ	58.60	3.34	MMS [0.01%]
***sgs11Δ tdp1Δ* (Obsv.)**	92.69	3.63	MMS [0.01%]
***sgs1Δ tdp1Δ* (Exp.)**	56.43	4.00	MMS [0.01%]
wild type	100.00	0.00	Etoposide [2mM]
rad27Δ	78.76	4.42	Etoposide [2mM]
mms4Δ	99.19	3.60	Etoposide [2mM]
***mms4Δ rad27Δ* (Obsv.)**	96.10	1.38	Etoposide [2mM]
***mms4Δ rad27Δ* (Exp.)**	78.12	7.22	Etoposide [2mM]

Interactions	Fitness%	SD	DDA [concentration]
wild type	100.00	0.00	Camptothecin [50μM]
tdp1Δ	93.55	1.12	Camptothecin [50μM]
bub1Δ	44.02	0.53	Camptothecin [50μM]
***bub1Δ tdp1Δ* (Obsv.)**	92.64	2.22	Camptothecin [50μM]
***bub1 Δ tdp1Δ* (Exp.)**	41.19	0.77	Camptothecin [50μM]
wild type	100.00	0.00	Camptothecin [25μM]
rad27Δ	93.80	3.10	Camptothecin [25μM]
yen1Δ	105.95	1.62	Camptothecin [25μM]
***yen1Δ rad27Δ* (Obsv.)**	137.00	9.90	Camptothecin [25μM]
***yen1Δ rad27Δ* (Exp.)**	99.40	4.51	Camptothecin [25μM]
wild type	100.00	00.00	Camptothecin [25μM]
rad27Δ	73.65	3.15	Camptothecin [25μM]
nhp6Δ	88.65	3.48	Camptothecin [25μM]
***nhp6Δ rad27Δ* (Obsv.)**	103.37	5.69	Camptothecin [25μM]
***nhp6Δ rad27Δ* (Exp.)**	65.35	5.18	Camptothecin [25μM]
wild type	100.00	0.00	Cis-Platin [1.4mM]
tpp1Δ	94.73	0.63	Cis-Platin [1.4mM]
sae1Δ	60.28	1.86	Cis-Platin [1.4mM]
***sae2Δ tpp1Δ* (Obsv.)**	110.91	2.10	Cis-Platin [1.4mM]
***sae2Δ tpp1Δ* (Exp.)**	57.10	1.40	Cis-Platin [1.4mM]
wild type	100.00	0.00	Cis-Platin [1.4mM]
tdp1Δ	111.38	12.68	Cis-Platin [1.4mM]
sae1Δ	90.22	2.07	Cis-Platin [1.4mM]
***sae2Δ tdp1Δ* (Obsv.)**	152.25	3.68	Cis-Platin [1.4mM]
***sae2Δ tdp1Δ* (Exp.)**	100.47	11.48	Cis-Platin [1.4mM]
wild type	100.00	0.00	Cis-Platin [1.4mM]
tpp1Δ	96.25	2.47	Cis-Platin [1.4mM]
yku70Δ	58.60	3.34	Cis-Platin [1.4mM]
***yku70Δ tpp1Δ* (Obsv.)**	92.69	3.63	Cis-Platin [1.4mM]
***yku70Δ tpp1Δ* (Exp.)**	56.43	4.00	Cis-Platin [1.4mM]
wild type	100.00	0.00	Cis-Platin [1.4mM]
tpp1Δ	93.55	1.12	Cis-Platin [1.4mM]
dun1Δ	44.02	0.53	Cis-Platin [1.4mM]
***dun1Δ tpp1Δ* (Obsv.)**	92.64	2.22	Cis-Platin [1.4mM]
***dun1Δ tpp1Δ* (Exp.)**	41.19	0.77	Cis-Platin [1.4mM]
wild type	100.00	0.00	Cis-Platin [1.4mM]
tdp1Δ	94.02	3.83	Cis-Platin [1.4mM]
dun1Δ	41.23	1.22	Cis-Platin [1.4mM]
***dun1Δ tdp1Δ* (Obsv.)**	68.75	3.34	Cis-Platin [1.4mM]
***dun1Δ tdp1Δ* (Exp.)**	38.79	2.43	Cis-Platin [1.4mM]

Table 5: Fitness calculations relative to the wild type strain to identify PS interactions by using the area under the curve. The calculation of expected and observed fitness to identify 19 PS interactions under the application of different DDAs.

Interactions	Fitness%	SD	DDA [concentration]
wild type	100.00	0.00	Bleomycin [2.5µg/ml]
yku70Δ	105.88	6.11	Bleomycin [2.5µg/ml]
rad52Δ	61.93	5.50	Bleomycin [2.5µg/ml]
***yku70Δ rad52Δ* (Obsv.)**	39.50	2.80	Bleomycin [2.5µg/ml]
***yku70Δ rad52Δ* (Exp.)**	65.74	8.70	Bleomycin [2.5µg/ml]
wild type	100.00	0.00	Bleomycin [2.5µg/ml]
yku70Δ	73.02	3.17	Bleomycin [2.5µg/ml]
mre11Δ	42.39	2.10	Bleomycin [2.5µg/ml]
***yku70Δ mre11Δ* (Obsv.)**	15.05	3.75	Bleomycin [2.5µg/ml]
***yku70Δ mre11Δ* (Exp.)**	30.95	2.92	Bleomycin [2.5µg/ml]
wild type	100.00	0.00	Bleomycin [2.5µg/ml]
tpp1Δ	101.62	1.99	Bleomycin [2.5µg/ml]
xrs2Δ	71.84	7.26	Bleomycin [2.5µg/ml]
***xrs2Δ tpp1Δ* (Obsv.)**	53.88	0.68	Bleomycin [2.5µg/ml]
***xrs2Δ tpp1Δ* (Exp.)**	73.00	8.32	Bleomycin [2.5µg/ml]
wild type	100.00	0.00	Bleomycin [2.5µg/ml]
rad52Δ	40.12	1.07	Bleomycin [2.5µg/ml]
mre11Δ	32.32	1.23	Bleomycin [2.5µg/ml]
***mre11Δ rad52Δ* (Obsv.)**	6.77	0.75	Bleomycin [2.5µg/ml]
***mre11Δ rad52Δ* (Exp.)**	12.96	1.15	Bleomycin [2.5µg/ml]
wild type	100.00	0.00	Bleomycin [2.5µg/ml]
tpp1Δ	94.00	3.84	Bleomycin [2.5µg/ml]
rad52Δ	35.39	1.22	Bleomycin [2.5µg/ml]
***rad52Δ tpp1Δ* (Obsv.)**	68.24	3.36	Bleomycin [2.5µg/ml]
***rad52Δ tpp1Δ* (Exp.)**	33.26	2.45	Bleomycin [2.5µg/ml]

Table 6: AUC calculations for PS and SC interactions in Figure 9

Bibliography

Adhikari, S., Choudhury, S., Mitra, P. S., Dubash, J. J., Sajankila, S. P., & Roy, R. (2008). Targeting base excision repair for chemosensitization. *Anti-cancer agents in medicinal chemistry*, *8*(4), 351–357.

Alvaro, D., Lisby, M., & Rothstein, R. (2007). Genome-Wide Analysis of Rad52 Foci Reveals Diverse Mechanisms Impacting Recombination. *PLoS Genet*, *3*(12), e228.

Balakrishnan, L., & Bambara, R. A. (2013). Flap Endonuclease 1. *Annual Review of Biochemistry*, *82*(1), 119–138. doi:10.1146/annurev-biochem-072511-122603

Bernstein, N. K., Karimi-Busheri, F., Rasouli-Nia, A., Mani, R., Dianov, G., Glover, J. N. M., & Weinfeld, M. (2008). Polynucleotide kinase as a potential target for enhancing cytotoxicity by ionizing radiation and topoisomerase I inhibitors. *Anti-cancer agents in medicinal chemistry*, *8*(4), 358–367.

Bonora, A., & Mares, D. (1982). A simple colorimetric method for detecting cell viability in cultures of eukaryotic microorganisms. *Current Microbiology*, *7*(4), 217–221.

Boone, C., Bussey, H., & Andrews, B. J. (2007). Exploring genetic interactions and networks with yeast. *Nature reviews. Genetics*, *8*(6), 437–449.

Bouwman, P., & Jonkers, J. (2012). The effects of deregulated DNA damage signalling on cancer chemotherapy response and resistance. *Nature reviews. Cancer*, *12*(9), 587–598.

Bryant, H. E., Schultz, N., Thomas, H. D., Parker, K. M., Flower, D., Lopez, E., Helleday, T. (2005). Specific killing of BRCA2-deficient tumours with inhibitors of poly(ADP-ribose) polymerase. *Nature*, *434*(7035), 913–917.

Cahill, D. P., Kinzler, K. W., Vogelstein, B., & Lengauer, C. (1999). Genetic instability and darwinian selection in tumours. *Trends in Cell Biology*, *9*(12), M57–M60.

Calabrese, C. R., Almassy, R., Barton, S., Batey, M. A., Calvert, A. H., Canan-Koch, S., Curtin, N. J. (2004). Anticancer chemosensitization and radiosensitization by the novel poly(ADP-ribose) polymerase-1 inhibitor AG14361. *Journal of the National Cancer Institute*, *96*(1), 56–67.

Chan, D. A., & Giaccia, A. J. (2011). Harnessing synthetic lethal interactions in anticancer drug discovery. *Nature reviews. Drug discovery*, *10*(5), 351–364.

Charames, G. S., & Bapat, B. (2003). Genomic instability and cancer. *Current molecular medicine*, *3*(7), 589–596.

Cherry, J. M., Adler, C., Ball, C., Chervitz, S. A., Dwight, S. S., Hester, E. T., Botstein, D. (1998). SGD: Saccharomyces Genome Database. *Nucleic Acids Research*, *26*(1), 73–79.

Dixon, S. J., Costanzo, M., Baryshnikova, A., Andrews, B., & Boone, C. (2009). Systematic Mapping of Genetic Interaction Networks. *Annual Review of Genetics*, *43*(1), 601–625.

Doles, J., Oliver, T. G., Cameron, E. R., Hsu, G., Jacks, T., Walker, G. C., & Hemann, M. T. (2010). Suppression of Rev3, the catalytic subunit of Pol{zeta}, sensitizes drug-resistant lung tumors to chemotherapy. *Proceedings of the National Academy of Sciences of the United States of America*, *107*(48), 20786–20791. doi:10.1073/pnas.1011409107

Donawho, C. K., Luo, Y., Luo, Y., Penning, T. D., Bauch, J. L., Bouska, J. J., Frost, D. J. (2007). ABT-888, an Orally Active Poly(ADP-Ribose) Polymerase Inhibitor that Potentiates DNA-Damaging Agents in Preclinical Tumor Models. *Clinical Cancer Research*, *13*(9), 2728–2737. doi:10.1158/1078-0432.CCR-06-3039

Evers, B., Drost, R., Schut, E., Bruin, M. de, Burg, E. van der, Derksen, P. W. B., Jonkers, J. (2008). Selective Inhibition of BRCA2-Deficient Mammary Tumor Cell Growth by

AZD2281 and Cisplatin. *Clinical Cancer Research*, *14*(12), 3916–3925. doi:10.1158/1078-0432.CCR-07-4953

Farmer, H., McCabe, N., Lord, C. J., Tutt, A. N. J., Johnson, D. A., Richardson, T. B., Ashworth, A. (2005). Targeting the DNA repair defect in BRCA mutant cells as a therapeutic strategy. *Nature*, *434*(7035), 917–921.

Ferrari, E., Lucca, C., & Foiani, M. (2010). A lethal combination for cancer cells: synthetic lethality screenings for drug discovery. *European journal of cancer (Oxford, England: 1990)*, *46*(16), 2889–2895.

Fishel, R., Lescoe, M. K., Rao, M. R., Copeland, N. G., Jenkins, N. A., Garber, J., Kolodner, R. (1993). The human mutator gene homolog MSH2 and its association with hereditary nonpolyposis colon cancer. *Cell*, *75*(5), 1027–1038.

Fong, P. C., Boss, D. S., Yap, T. A., Tutt, A., Wu, P., Mergui-Roelvink, M., de Bono, J. S. (2009). Inhibition of poly(ADP-ribose) polymerase in tumors from BRCA mutation carriers. *The New England journal of medicine*, *361*(2), 123–134.

Freschauf, G. K., Karimi-Busheri, F., Ulaczyk-Lesanko, A., Mereniuk, T. R., Ahrens, A., Koshy, J. M., Weinfeld, M. (2009). Identification of a small molecule inhibitor of the human DNA repair enzyme polynucleotide kinase/phosphatase. *Cancer research*, *69*(19), 7739–7746.

Gatenby, R. A., & Vincent, T. L. (2003). An Evolutionary Model Of Carcinogenesis. *Cancer Research*, *63*(19), 6212–6220.

Gietz, R. D., Schiestl, R. H., Willems, A. R., & Woods, R. A. (1995). Studies on the transformation of intact yeast cells by the LiAc/SS-DNA/PEG procedure. *Yeast (Chichester, England)*, *11*(4), 355–360.

Hahn, W. C., & Weinberg, R. A. (2002). Modelling the molecular circuitry of cancer. *Nature reviews. Cancer*, *2*(5), 331–341.

Hanahan, D, & Weinberg, R. A. (2000). The hallmarks of cancer. *Cell*, *100*(1), 57–70.

Hanahan, Douglas, & Weinberg, R. A. (2011). Hallmarks of cancer: the next generation. *Cell*, *144*(5), 646–674.

Hanks, S., Coleman, K., Reid, S., Plaja, A., Firth, H., Fitzpatrick, D., Rahman, N. (2004). Constitutional aneuploidy and cancer predisposition caused by biallelic mutations in BUB1B. *Nature genetics*, *36*(11), 1159–1161.

Heinicke, S., Livstone, M. S., Lu, C., Oughtred, R., Kang, F., Angiuoli, S. V., Dolinski, K. (2007). The Princeton Protein Orthology Database (P-POD): A Comparative Genomics Analysis Tool for Biologists. *PLoS ONE*, *2*(8), e766.

Helleday, T., Petermann, E., Lundin, C., Hodgson, B., & Sharma, R. A. (2008). DNA repair pathways as targets for cancer therapy. *Nature reviews. Cancer*, *8*(3), 193–204.

Huang, S. N., Pommier, Y., & Marchand, C. (2011). Tyrosyl-DNA Phosphodiesterase 1 (Tdp1) inhibitors. *Expert opinion on therapeutic patents*, *21*(9), 1285–1292.

Huh, W.-K., Falvo, J. V., Gerke, L. C., Carroll, A. S., Howson, R. W., Weissman, J. S., & O'Shea, E. K. (2003). Global analysis of protein localization in budding yeast. *Nature*, *425*(6959), 686–691.

Kaelin, W. G., Jr. (2005). The concept of synthetic lethality in the context of anticancer therapy. *Nature reviews. Cancer*, *5*(9), 689–698.

Kitagawa, K., & Hieter, P. (2001). Evolutionary conservation between budding yeast and human kinetochores. *Nature reviews. Molecular cell biology*, *2*(9), 678–687.

Kolodner, R D. (1995). Mismatch repair: mechanisms and relationship to cancer susceptibility. *Trends in biochemical sciences*, *20*(10), 397–401.

Kolodner, Richard D., Putnam, C. D., & Myung, K. (2002). Maintenance of Genome Stability in Saccharomyces cerevisiae. *Science*, *297*(5581), 552–557.

Larsen, E., Gran, C., Saether, B. E., Seeberg, E., & Klungland, A. (2003). Proliferation Failure and Gamma Radiation Sensitivity of Fen1 Null Mutant Mice at the Blastocyst Stage. *Molecular and Cellular Biology*, *23*(15), 5346–5353.

Le Meur, N., & Gentleman, R. (2008). Modeling synthetic lethality. *Genome Biology*, *9*(9), R135.

Leach, F. S., Nicolaides, N. C., Papadopoulos, N., Liu, B., Jen, J., Parsons, R., Nyström-Lahti, M. (1993). Mutations of a mutS homolog in hereditary nonpolyposis colorectal cancer. *Cell*, *75*(6), 1215–1225.

Lengauer, C., Kinzler, K. W., & Vogelstein, B. (1997). Genetic instability in colorectal cancers. *Nature*, *386*(6625), 623–627.

Lieber, M. R., Ma, Y., Pannicke, U., & Schwarz, K. (2004). The mechanism of vertebrate nonhomologous DNA end joining and its role in V(D)J recombination. *DNA repair*, *3*(8-9), 817–826. doi:10.1016/j.dnarep.2004.03.015

Liu, Y., Kao, H.-I., & Bambara, R. A. (2004). Flap endonuclease 1: a central component of DNA metabolism. *Annual review of biochemistry*, *73*, 589–615.

Loeb, K. R., & Loeb, L. A. (2000). Significance of multiple mutations in cancer. *Carcinogenesis*, *21*(3), 379–385.

Longhese, M. P., Bonetti, D., Manfrini, N., & Clerici, M. (2010). Mechanisms and regulation of DNA end resection. *The EMBO Journal*, *29*(17), 2864–2874. doi:10.1038/emboj.2010.165

Luo, J., Emanuele, M. J., Li, D., Creighton, C. J., Schlabach, M. R., Westbrook, T. F., Elledge, S. J. (2009). A genome-wide RNAi screen identifies multiple synthetic lethal interactions with the Ras oncogene. *Cell*, *137*(5), 835–848.

Mani, R., St.Onge, R. P., Hartman, J. L., Giaever, G., & Roth, F. P. (2008). Defining genetic interaction. *Proceedings of the National Academy of Sciences*, *105*(9), 3461–3466.

Martin, L. P., Hamilton, T. C., & Schilder, R. J. (2008). Platinum Resistance: The Role of DNA Repair Pathways. *Clinical Cancer Research*, *14*(5), 1291–1295.

McLellan, J. L., O'Neil, N. J., Barrett, I., Ferree, E., van Pel, D. M., Ushey, K., Hieter, P. (2012). Synthetic Lethality of Cohesins with PARPs and Replication Fork Mediators. *PLoS Genetics*, *8*(3).

McLellan, J., O'Neil, N., Tarailo, S., Stoepel, J., Bryan, J., Rose, A., & Hieter, P. (2009). Synthetic lethal genetic interactions that decrease somatic cell proliferation in Caenorhabditis elegans identify the alternative RFC CTF18 as a candidate cancer drug target. *Molecular biology of the cell*, *20*(24), 5306–5313.

McManus, K. J., Barrett, I. J., Nouhi, Y., & Hieter, P. (2009). Specific synthetic lethal killing of RAD54B-deficient human colorectal cancer cells by FEN1 silencing. *Proceedings of the National Academy of Sciences of the United States of America*, *106*(9), 3276–3281.

Mereniuk, T. R., Maranchuk, R. A., Schindler, A., Penner-Chea, J., Freschauf, G. K., Hegazy, S., Weinfeld, M. (2012). Genetic screening for synthetic lethal partners of polynucleotide

kinase/phosphatase: potential for targeting SHP-1-depleted cancers. *Cancer research*, *72*(22), 5934–5944.

Negrini, S., Gorgoulis, V. G., & Halazonetis, T. D. (2010). Genomic instability an evolving hallmark of cancer. *Nature reviews. Molecular cell biology*, *11*(3), 220–228.

Nitiss, K. C., Malik, M., He, X., White, S. W., & Nitiss, J. L. (2006). Tyrosyl-DNA phosphodiesterase (Tdp1) participates in the repair of Top2-mediated DNA damage. *Proceedings of the National Academy of Sciences of the United States of America*, *103*(24), 8953–8958.

Pel, D. M. van, Stirling, P. C., Minaker, S. W., Sipahimalani, P., & Hieter, P. (2013). Saccharomyces cerevisiae Genetics Predicts Candidate Therapeutic Genetic Interactions at the Mammalian Replication Fork. *G3: Genes|Genomes|Genetics*, *3*(2), 273–282.

Podlaha, O., Riester, M., De, S., & Michor, F. (2012). Evolution of the cancer genome. *Trends in genetics : TIG*, *28*(4), 155–163.

Pouliot, J. J., Yao, K. C., Robertson, C. A., & Nash, H. A. (1999). Yeast Gene for a Tyr-DNA Phosphodiesterase that Repairs Topoisomerase I Complexes. *Science*, *286*(5439), 552–555.

Rajagopalan, H., Nowak, M. A., Vogelstein, B., & Lengauer, C. (2003). The significance of unstable chromosomes in colorectal cancer. *Nature reviews. Cancer*, *3*(9), 695–701.

Ringvoll, J., Uldal, L., Roed, M. A., Reite, K., Baynton, K., Klungland, A., & Eide, L. (2007). Mutations in the RAD27 and SGS1 genes differentially affect the chronological and replicative lifespan of yeast cells growing on glucose and glycerol. *FEMS yeast research*, *7*(6), 848–859.

Rottenberg, S., Jaspers, J. E., Kersbergen, A., Burg, E. van der, Nygren, A. O. H., Zander, S. A. L., Jonkers, J. (2008). High sensitivity of BRCA1-deficient mammary tumors to the PARP inhibitor AZD2281 alone and in combination with platinum drugs. *Proceedings of the National Academy of Sciences*, *105*(44), 17079–17084. doi:10.1073/pnas.0806092105

Sabourin, M., Nitiss, J. L., Nitiss, K. C., Tatebayashi, K., Ikeda, H., & Osheroff, N. (2003). Yeast recombination pathways triggered by topoisomerase II- mediated DNA breaks. *Nucleic Acids Research*, *31*(15), 4373–4384.

Samejima, I., Matsumoto, T., Nakaseko, Y., Beach, D., & Yanagida, M. (1993). Identification of seven new cut genes involved in Schizosaccharomyces pombe mitosis. *Journal of Cell Science*, *105*(1), 135–143.

Schaerer, F., Morgan, G., Winey, M., & Philippsen, P. (2001). Cnm67p Is a Spacer Protein of the Saccharomyces cerevisiae Spindle Pole Body Outer Plaque. *Molecular Biology of the Cell*, *12*(8), 2519–2533.

Scherens, B., & Goffeau, A. (2004). The uses of genome-wide yeast mutant collections. *Genome Biology*, *5*(7), 229.

Schvartzman, J.-M., Sotillo, R., & Benezra, R. (2010). Mitotic chromosomal instability and cancer: mouse modelling of the human disease. *Nature reviews. Cancer*, *10*(2), 102–115.

Shaheen, M., Allen, C., Nickoloff, J. A., & Hromas, R. (2011). Synthetic lethality: exploiting the addiction of cancer to DNA repair. *Blood*, *117*(23), 6074–6082.

Shih, I. M., Zhou, W., Goodman, S. N., Lengauer, C., Kinzler, K. W., & Vogelstein, B. (2001). Evidence that genetic instability occurs at an early stage of colorectal tumorigenesis. *Cancer research*, *61*(3), 818–822.

Sjöblom, T., Jones, S., Wood, L. D., Parsons, D. W., Lin, J., Barber, T. D., Velculescu, V. E. (2006). The Consensus Coding Sequences of Human Breast and Colorectal Cancers. *Science*, *314*(5797), 268–274.

Stirling, P. C., Bloom, M. S., Solanki-Patil, T., Smith, S., Sipahimalani, P., Li, Z., Hieter, P. (2011). The Complete Spectrum of Yeast Chromosome Instability Genes Identifies Candidate CIN Cancer Genes and Functional Roles for ASTRA Complex Components. *PLoS Genet*, *7*(4), e1002057.

Stirling, P. C., Chan, Y. A., Minaker, S. W., Aristizabal, M. J., Barrett, I., Sipahimalani, P., Hieter, P. (2012). R-loop-mediated genome instability in mRNA cleavage and polyadenylation mutants. *Genes & development*, *26*(2), 163–175.

Stratton, M. R., Campbell, P. J., & Futreal, P. A. (2009). The cancer genome. *Nature*, *458*(7239), 719–724.

Tarailo, M., Tarailo, S., & Rose, A. M. (2007). Synthetic Lethal Interactions Identify Phenotypic "Interologs" of the Spindle Assembly Checkpoint Components. *Genetics*, *177*(4), 2525–2530.

Tong, A. H. Y. (2001). Systematic Genetic Analysis with Ordered Arrays of Yeast Deletion Mutants. *Science*, *294*(5550), 2364–2368.

Van Pel, D. M., Barrett, I. J., Shimizu, Y., Sajesh, B. V., Guppy, B. J., Pfeifer, T., Hieter, P. (2013). An Evolutionarily Conserved Synthetic Lethal Interaction Network Identifies FEN1 as a Broad-Spectrum Target for Anticancer Therapeutic Development. *PLoS Genetics*, *9*(1).

Vance, J R, & Wilson, T. E. (2001). Uncoupling of 3’-phosphatase and 5’-kinase functions in budding yeast. Characterization of Saccharomyces cerevisiae DNA 3’-phosphatase (TPP1). *The Journal of biological chemistry*, *276*(18), 15073–15081.

Vance, John R., & Wilson, T. E. (2002). Yeast Tdp1 and Rad1-Rad10 function as redundant pathways for repairing Top1 replicative damage. *Proceedings of the National Academy of Sciences*, *99*(21), 13669–13674.

Vogelstein, B., & Kinzler, K. W. (2004). Cancer genes and the pathways they control. *Nature medicine*, *10*(8), 789–799.

Weinert, T. A., & Hartwell, L. H. (1990). Characterization of RAD9 of Saccharomyces cerevisiae and evidence that its function acts posttranslationally in cell cycle arrest after DNA damage. *Molecular and Cellular Biology*, *10*(12), 6554–6564.

Weinfeld, M., Mani, R. S., Abdou, I., Acetuno, R. D., & Glover, J. N. M. (2011). Tidying up loose ends: the role of polynucleotide kinase/phosphatase in DNA strand break repair. *Trends in biochemical sciences*, *36*(5), 262–271.

Xie, K., Doles, J., Hemann, M. T., & Walker, G. C. (2010). Error-prone translesion synthesis mediates acquired chemoresistance. *Proceedings of the National Academy of Sciences*, *107*(48), 20792–20797. doi:10.1073/pnas.1011412107